

SVENSKA INSTITUTEN I ATHEN OCH ROM  
INSTITUTUM ATHENIENSE ATQUE INSTITUTUM ROMANUM REGNI SUECIAE

---

# Opuscula

Annual of the Swedish Institutes at Athens and Rome

16  
2023

STOCKHOLM

#### EDITORIAL COMMITTEE

Prof. Henrik Gerding, Lund, Chairman  
Dr Lena Sjögren, Stockholm, Vice-chairman  
Mrs Kristina Björkstén Jersenius, Stockholm, Treasurer  
Dr Susanne Berndt, Stockholm, Secretary  
Prof. Denis Searby, Stockholm  
Prof. Christer Henriksén, Uppsala  
Dr Johan Eriksson, Uppsala  
Dr Lewis Webb, Gothenburg  
Prof. Gunnel Ekroth, Uppsala  
Mr Julian Wareing, Stockholm  
Dr Ulf R. Hansson, Rome  
Dr Jenny Wallensten, Athens

#### EDITOR

Dr Julia Habetzeder

#### SECRETARY'S & EDITOR'S ADDRESS

Department of Archaeology and Classical Studies  
Stockholm University  
106 91 Stockholm, Sweden  
secretary@ecsi.se | editor@ecsi.se

#### DISTRIBUTOR

Eddy.se AB  
Box 1310  
621 24 Visby, Sweden

For general information, see <https://ecsi.se>  
For subscriptions, prices and delivery, see <https://ecsi.bokorder.se>  
Published with the aid of a grant from The Swedish Research Council (2020-01217)  
The English text was revised by Rebecca Montague, Hindon, Salisbury, UK

The text of this work is licenced under a Creative Commons Attribution 4.0 International Licence (CC BY 4.0). To view a copy of this licence, visit <https://creativecommons.org/licenses/by/4.0/>. All figures are reproduced with the permission of the rights holders acknowledged in captions. The figures are expressly excluded from the CC BY license covering the text; they may not be reproduced, copied, transmitted, or manipulated without consent from the owners, who reserve all rights.

*Opuscula* is a peer reviewed journal. Contributions to *Opuscula* should be sent to the Secretary of the Editorial Committee before 1 November every year. Contributors are requested to include an abstract summarizing the main points and principal conclusions of their article. For style of references to be adopted, see <https://ecsi.se>. Books for review should be sent to the Secretary of the Editorial Committee.

ISSN 2000-0898

ISBN 978-91-977799-5-1

© Svenska Institutet i Athen and Svenska Institutet i Rom

Printed by PrintBest (Viljandi, Estonia) via Italgraf Media AB (Stockholm, Sweden) 2023

Cover illustration from Robin Rönnlund in this volume, p. 123, fig. 6. Photograph by Robin Rönnlund. Courtesy of Ministry of Culture and Sports—Directorate for the Administration of the National Archive of Monuments—Department for the Administration of the Historical Archive of Antiquities and Restorations.

# The New Swedish Cyprus Expedition (The Söderberg Expedition): Excavations at Hala Sultan Tekke autumn 2021 and spring 2022

## Preliminary results

### Abstract

In 2021 and 2022, the 13th and 14th seasons of excavations at the Late Bronze Age site of Hala Sultan Tekke were carried out in Area A, and as a result of these investigations numerous tombs were found. These tombs were threatened by farming. Four magnetic anomalies, indicated in the 2017 survey magnetometer map, were investigated. They represent three tombs, L198, TT, and UU, and the probable Offering Pit SS-S. The minimum number of individuals (MNI) in Pit Tomb L198, which contains only secondary burials, is six. They are associated with 21 ceramic vessels of which a few were imported from Anatolia. Chamber Tomb TT was completely excavated and contained a minimum of 25 individuals and 78 objects. Among these are 47 ceramic vessels of which a few are from the Mycenaean sphere of culture. Other mortuary gifts are various objects of metal, faience, carnelian, haematite, and rock crystal in addition to three scarabs. The incompletely excavated large (Chamber?) Tomb UU contained, so far, a minimum of 19 individuals and 140 objects. They comprise 124 ceramic vessels including numerous Late Hellenic, Late Minoan, and Anatolian pottery. Other finds are bronze and gold jewellery, the latter including a diadem, and a duck-shaped ivory box from the same context as Egyptian-imported vessels of calcite. None of the tombs and the offering pit, which can all be roughly dated to the 14th century BC, were looted. The special arrangements of the human bones in Chamber Tomb TT and the multitude of imported materials in Tomb UU offer additional insights into complex Late Cypriot mortuary practices and the far-reaching interregional connections of the urban élites of Hala Sultan Tekke.\*

*Keywords:* Cyprus, funerary archaeology, Hala Sultan Tekke, Late Bronze Age, mortuary practices

<https://doi.org/10.30549/opathrom-16-02>

### Introduction

In 2021 and 2022, the 13th and 14th seasons of excavation at the Late Bronze Age harbour city of Hala Sultan Tekke (Dromoloxia *Vyzakia*) were carried out in Area A, which represents the extramural cemetery of the site (*Fig. 1*).

The excavations of the large Tomb SS, immediately to the south of Tomb RR, began in 2020.<sup>1</sup> At the end of the spring 2021 campaign, the outlines of a feature, which later turned out to represent a pit tomb (Pit Tomb L198), were observed on the surface of the floor in the northern part of Tomb SS.

---

\* Acknowledgements: The expedition would like to express thanks for the support given by the Department of Antiquities of Cyprus (DAC), headed by its director Dr Marina Solomidou-Ieronymidou, and its personnel including archaeological officer Dr Anna Satraki, and the staff of the Larnaca Archaeological Museum. H.E. Anders Hagelberg, ambassador at the Swedish Embassy in Nicosia, showed great interest in the expedition and supported it in many ways for which we are very grateful. Andreani Papageorgiou and Christodoulos Sofokleous acted most proficiently as the expedition's surveyors, and Mr Petros Georgiou, a former employee of the DAC, and Mrs Dina Georgiou admirably provided the necessary logistical support. Professors Kirsi O. Lorentz and Sorin Hermon and their teams from the Cyprus Institute in Nicosia contributed efficiently to the successful work in the field and laboratories. Indispensable funding was once again gratefully received from the Torsten Söderberg Foundation. We are also much obliged to the Enbom's Foundation at the Royal Swedish Academy of Letters, History and Antiquities, and to The Royal Society of Arts and Sciences in Gothenburg for their generous sponsorships. The board of the association of the Friends of the Swedish Cyprus Expedition lent their kind support. Under the supervision of the directors of the excavations Professor Peter M. Fischer and Dr Teresa Bürge assisted by Dr Rainer Feldbacher, with the additional supervision of professors Kirsi O. Lorentz and Sorin Hermon, the fieldwork and material studies were carried out by Juuli Ahola, Maria Nectaria Antoniou, Lucía Avial Chicharro, Natalie M. Branca, Bianca Casa, Dr Svetlana Gasanova, Elena Iakovou, Loizos Ioannou, Panagiotis Ioannou, Sila Kayalp, Yuko Miyauchi, Rahaf Orabi, Magdalena Pelc, Elena Peri, Tom Stavrou, Jacek Tracz and Dr Valentina Vassallo. The animal bones and molluscs were kindly studied by Dr David Reese and the scarabs by Dr Jürg Egger. The restoration of ceramic vessels was professionally carried out by Constantina Hadjivasili.

<sup>1</sup> Fischer & Bürge 2021; 2022.



Fig. 1. Overview of Hala Sultan Tekke, Area A, with the features excavated in 2022 circled in red (by M. Al-Bataineh, modified by P.M. Fischer and T. Bürge).

On that occasion, the pit tomb was not further exposed but appropriately protected at the end of the spring 2021 campaign, and in November 2021 it was completely excavated. Also in 2021, just to the south of Tomb SS, features were observed that indicated the presence of another tomb. This area, which was labelled Pit SS-S, was further investigated in 2022. Chamber Tomb TT, just north of the Tomb RR and inside an already fenced area,<sup>2</sup> was precisely located with the aid of the magnetometer map from 2017 and completely excavated in 2022.

During a surface survey in May 2022, an area approximately 100 m to the north-west of Chamber Tomb TT revealed a concentration of Late Cypriot and imported sherds and human bones in a recently harvested field (regarding chronology, see *Table 1*). These objects were obviously disturbed and spread *ex situ* by the plough. Consequently, the co-ordinates of these findings were linked to the corresponding area on the magnetometer map, where a large and distinct magnetic anomaly is visible. Provisionally, the area of the magnetic anomaly was termed “Tomb UU” and, in agreement with the

local farmer, a 20 × 15 m-large area was fenced off. A tomb of considerable size was exposed during the 2022 fieldwork.

Thus, the current preliminary report concentrates on the material evidence from Pit Tomb L198, Offering Pit SS-S, and Tombs TT and UU.

## Pit Tomb L198 and associated L150

BY PETER M. FISCHER & TERESA BÜRGE

The level of the floor of Tomb SS is *c.* 11 masl.<sup>3</sup> At the end of the spring 2021 campaign, a well-demarcated concentration of pottery (L150) was found in the northern part of Tomb SS between 11.27 masl and 11.18 masl, *viz.* just above the floor level which in this area is 11.17 masl (*Fig. 2*). Cypriot-produced wares from L150 are jugs of Base-ring II, a Plain jug, and a White Shaved juglet, in addition to Mycenaean piriform jars (selected pottery in *Fig. 3*; *Table 2*).

After the removal of L150, the outlines of a feature, which later turned out to be Pit Tomb L198, were observed on the

<sup>2</sup> Fischer & Bürge 2019; 2020; 2021.

<sup>3</sup> Fischer & Bürge 2022, 29–50. All heights are in metres above mean sea level (masl).

Table 1. Comparative chronology of the Cypriot, Late Helladic, and Late Minoan cultures (E.g., Fischer & Bürge 2021, 98, table 1). The synchronization of the Late Helladic and Late Minoan periods is according to Malcolm H. Wiener (*pers. comm.* September 2021).

Late Cypriot (LC)	Late Helladic (LH)	Late Minoan (LM)	Approximate dates BC
IA1–2	I	IA	1630–1560
IB	IIA	IB	1560–1450
IIA(–B)	IIB	II	1450–1400
II(A–)B	IIIA1–2	IIIA1–2	1400–1300
IIC1–2	IIIB1–2	IIIB	1300–1200
IIIA1–2	IIIC	IIIC	1200–1100

surface of the floor approximately within the margins of the former L150. L197, a protecting layer of compact clay, was just above the entombments of L198. The circular tomb has a diameter of *c.* 0.8 m and a depth of 0.5 m (Figs. 4, 5). It contained the disarticulated remains of six (MNI) individuals, and numerous burial gifts (Table 3).<sup>4</sup> The latter comprises 21 vessels of fired clay but no additional finds of other materials except for some broken beads of faience. All vessels are intact/complete (see selection in Fig. 6), apart from two spindle bottles of Red Lustrous Wheel-made ware and a juglet of Base-ring I. Red Lustrous Wheel-made is the only imported pottery in the tomb.<sup>5</sup> The locally produced pottery comprises vessels of early White Slip II, Base-ring I, and Plain White. Base-ring II is absent. The White Slip II juglet (N542), which comes from the clay layer, is a type that is rare at the site (Fig. 6 second row right). It is decorated with vertical ladders and lattices on the body, horizontal lines on the neck, and wavy lines on the rim and handle. The interior of the flaring rim is also decorated with three bundles of four strokes. These patterns as well as the relatively fine, grey fabric, the thick light grey slip, and the carefully applied dark brown paint indicate an early date in the life span of White Slip II.<sup>6</sup> The large (early) White Slip II bowl (N556) is also rare at the site (Fig. 6 lowest row). Three shapes of Base-ring I juglets can be identified: rounded, carinated, and elongated, the later resembling the shape of early Red Lustrous Wheel-made examples, for instance, from Tomb LL (Fig. 6, N135, not to scale; 25 cm high).

<sup>4</sup> See Appendix 1.

<sup>5</sup> Recent studies, e.g., those by Kozal (2015; 2023) have convincingly demonstrated the Anatolian provenance of this ware.

<sup>6</sup> A very similar juglet with only slight variations in the decoration, perhaps from the same workshop, was exported to Alalakh; see Bergoffen 2005, 158, pl. 50:d, WE10.

Table 2. Locus 150 with concentration of pottery above Pit Tomb L198.

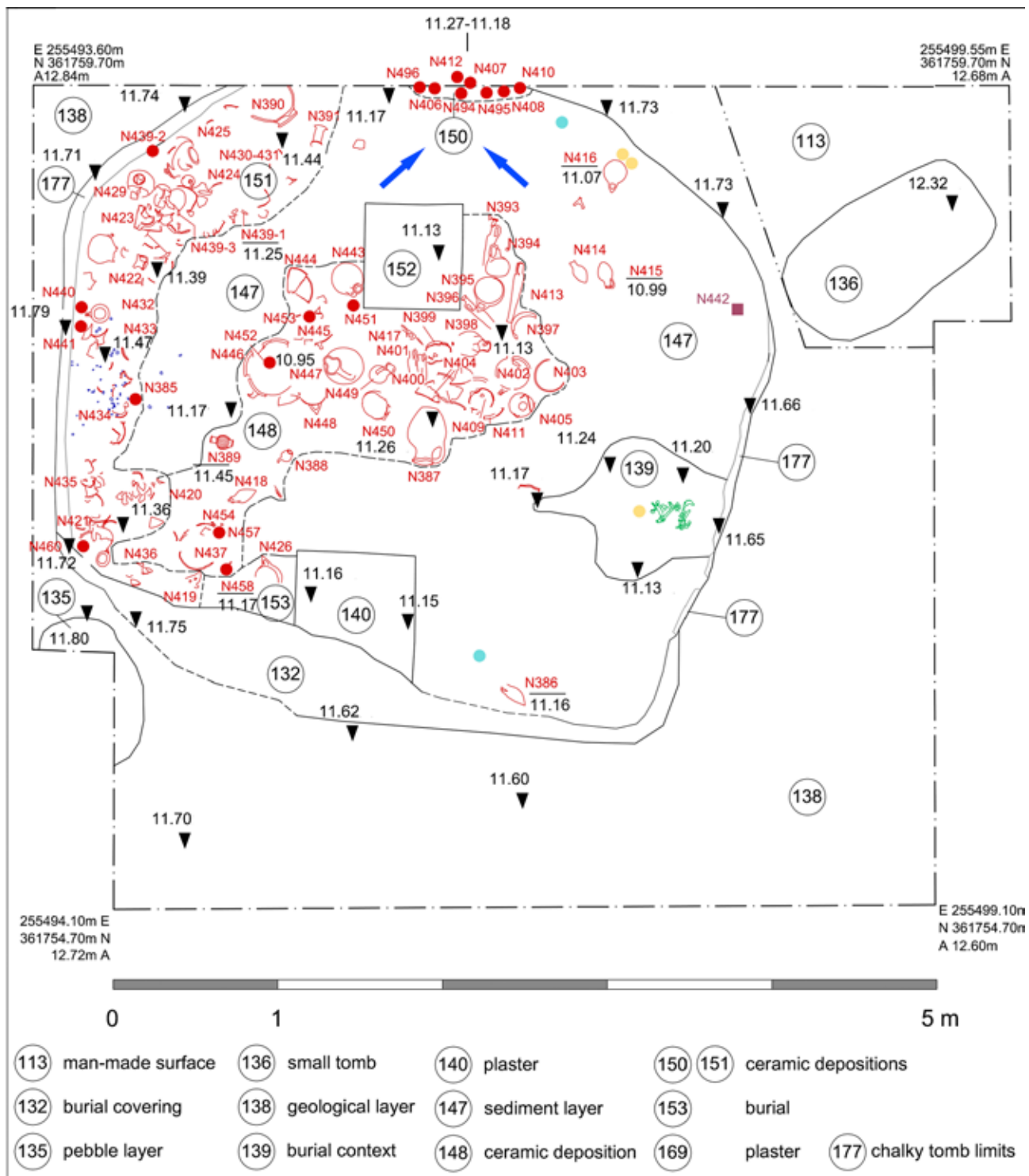
Find	Classification/Type	Shape/Object
412	Base-ring II	jug
408	Base-ring II	jug
495	Base-ring II	jug
407	Mycenaean	piriform jar
496	Mycenaean	piriform jar
406	Plain	jug
494	White Shaved	juglet
410	Undefined (fragmentary)	juglet

Table 3. Pottery from Pit Tomb L198.

Find	Classification/Type	Shape/Object
N547	Base-ring I	bowl
N562	Base-ring I	bowl
N548	Base-ring I	juglet
N551	Base-ring I	juglet
N553	Base-ring I	juglet
N558	Base-ring I	juglet
N559	Base-ring I	juglet
N560	Base-ring I	juglet
N563	Base-ring I	juglet
N564	Base-ring I	juglet
N561	Plain	juglet
N557	Plain	large jug
N549	Red Lustrous Wheel-made	spindle bottle
N550	Red Lustrous Wheel-made	spindle bottle
N552	Red Lustrous Wheel-made	spindle bottle
N554	White Painted VI	feeding juglet
N555	White Shaved	juglet
N565	White Shaved	juglet
N546	White Slip II	bowl
N542	White Slip II	juglet
N556	White Slip II	large bowl

## DISCUSSION OF PIT TOMB L198

The context of this small tomb, which was dug into the floor of the large Tomb SS, mirrors very well a secondary burial which certainly was completed on a single occasion. It seems that the builders of Tomb SS came across an older burial, prepared a pit, and buried incompletely gathered bones from somewhere else together with (some of?) the original burial gifts from the primary entombment. The pottery from the pit tomb, which does not contain any Mycenaean imports but only Anatolian-imported Red Lustrous Wheel-made vessels, suggests that the original tomb from which the pottery was



Hala Sultan Tekke	
date/ excavation period	04.05. - 12.05.2021
Tomb	SS
Loci	113, 132, 135, 136, 138, 139, 140, 147, 148, 150, 151, 153, 169, 177
geodetic system	EPSG 6312: CGRS93/ Cyprus Local Transverse Mercator,WGS 84
responsible	Anja Buhlke, info@anjabuhlke.de

— limit of excavation	● ceramics	N ↑
— limit of locus	☐ human bones	
- - - limit of locus, uncertain	■ metal	
○ stone	● bronze	
N320 number of single find	● silver, gold	
④ number of locus	● ivory	
	● faience	

Fig. 2. Tomb SS, floor level. L150 in the northern part of the tomb indicated with blue arrows. Pit Tomb L198 was beneath L150 (by A. Buhlke, modified by P.M. Fischer).



Fig. 3. Selected pottery from L150 (photographs by L. Avial Chicharro and B. Clark).



Fig. 4. Pit Tomb L198 below the layer of compact clay with disarticulated skeletal remains (photograph by P.M. Fischer).



Fig. 5. Large Plain White jug to the east of a broken cranium in Pit Tomb L198 (photograph by P.M. Fischer).

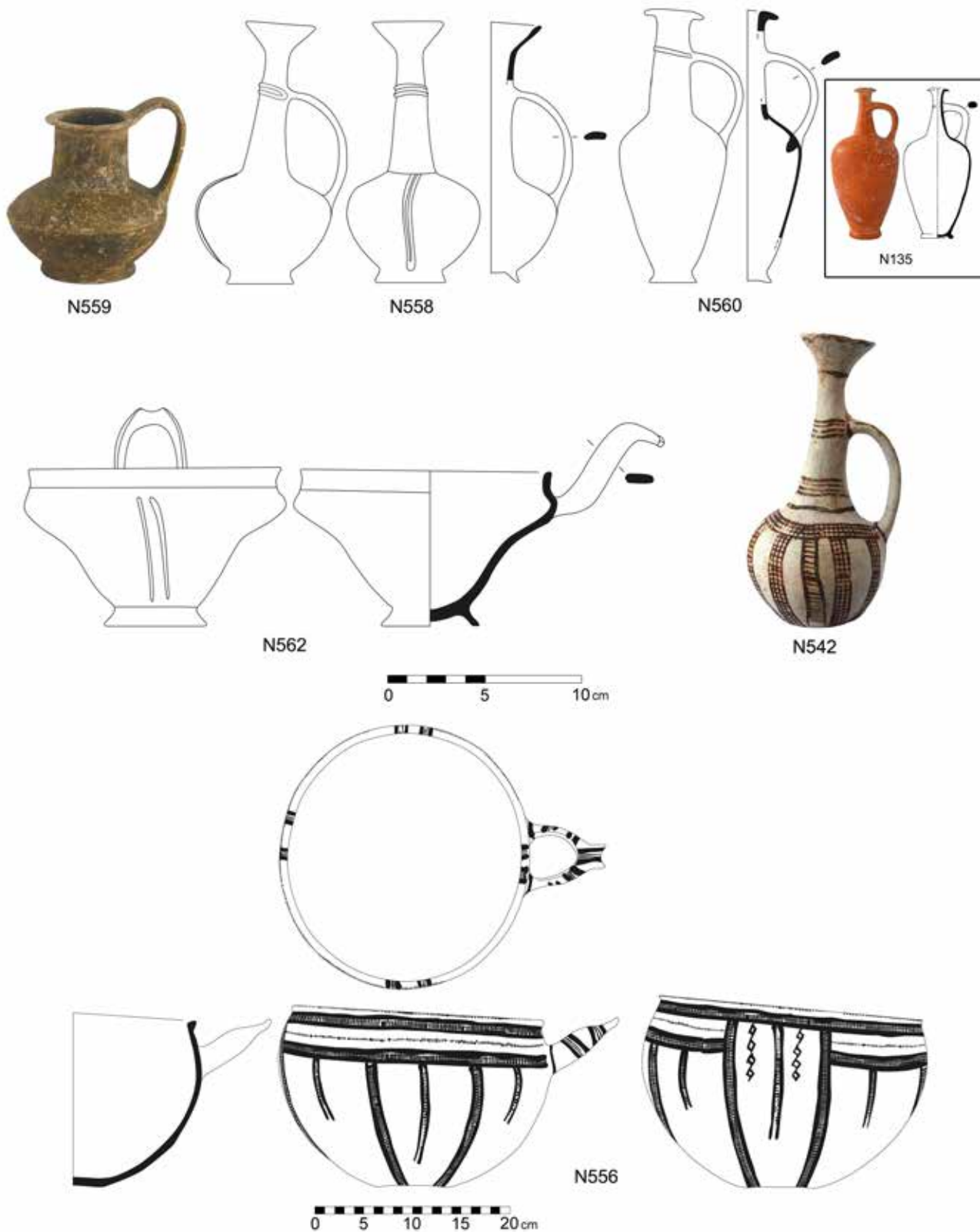


Fig. 6. Selection of pottery from Pit Tomb L198 below L150: Base-ring I juglets and bowl; Red Lustrous Wheel-made example from Tomb LL (not to scale within rectangle: 25 cm high); White Slip II juglet and large White Slip II (early) bowl (photographs by P.M. Fischer and T. Bürge, drawings by E. Peri).

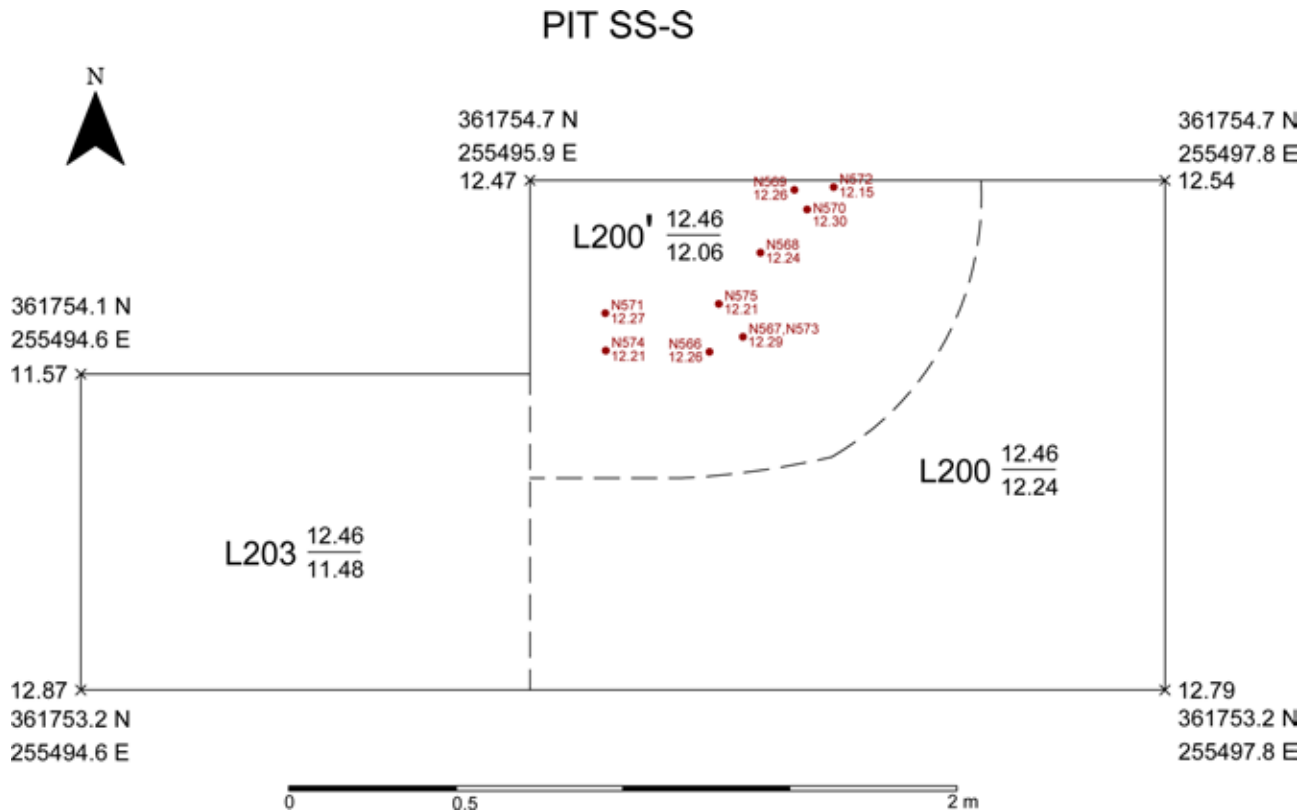


Fig. 7a. Plan of partly excavated Offering Pit SS-S with co-ordinates and outlines of pit indicated (by A. Papageorgiou and C. Sofokleous).

derived is somewhat older than Tomb SS. A date for the re-deposited contents of the pit tomb in the later part of LC IB, or the second half of the 15th century BC, can be suggested. In comparison, the earliest period of use of Tomb SS can also be dated to the later part of LC IB, but maybe at its end.<sup>7</sup> In contrast to the pit tomb, Tomb SS contained many Mycenaean vessels, none of which can be dated later than the end of LH IIIA2. Consequently, Tomb SS was in use from later LC IB to LC IIA(-B), i.e., over a period of approximately 125 years or from c. 1425–1300 BC.

## Offering Pit SS-S (south of Tomb SS; L126, L200, L200', L203)

BY PETER M. FISCHER & TERESA BÜRGE

In 2021, L126 was partly exposed just to the south of Tomb SS.<sup>8</sup> It contained a Base-ring I juglet (N241) which was originally interpreted as an indication of another tomb. After

protection, this area was further investigated at the beginning of the 2022 season (L200, L200', L203; Figs. 7a, b).

L200' in SS-S turned out to represent a pit that contained ten vessels of fired clay but no skeletal remains (Fig. 7a). The finds are all between 12.30 masl and 12.15 masl and a considerable distance higher than the floor of Tomb SS, which in the southern part is around 11.05 masl. There is no stratigraphical connection to Tomb SS, *viz.* these two features were dug separately. The pottery belongs to the standard Late Cypriot ceramic repertoire and consists of Base-ring, Monochrome, Plain White, White Shaved, and White Slip II wares but no imports (Table 4). Of particular note is the discovery of a miniature juglet of Plain Ware (N573) embedded into a white and soft, obviously organic, substance inside a White Slip II bowl (N567) (Fig. 8).<sup>9</sup>

## DISCUSSION OF OFFERING PIT SS-S

The absence of skeletal remains and the fact that most of the vessels have quite small dimensions suggest an offering pit for a child. Since Tomb SS contained child burials, it is most likely

<sup>7</sup> Fischer & Bürge 2022.

<sup>8</sup> Fischer & Bürge 2022.

<sup>9</sup> Analysis is under way.



Fig. 7b. Drone photograph taken 2022 looking south; in foreground Chamber Tomb TT (mid-season); in background Offering Pit SS-S (after partial excavation; photograph P.M. Fischer).



Fig. 8. Miniature juglet of Plain Ware (N573) embedded in an organic substance inside a White Slip II bowl (N567; photograph P.M. Fischer).

Table 4. Pottery from Offering Pit SS-S, Locus 200.

Find	Classification/Type	Shape/Object
N572	Base-ring	bowl
N575	Base-ring	bowl
N571	Base-ring	juglet
N574	Base-ring	juglet
N569	Monochrome	bowl
N573	Plain White	juglet, miniature
N566	White Shaved	juglet
N570	White Shaved	juglet
N567	White Slip II	bowl
N568	White Slip II	bowl

that the child, for whom the pottery was offered, was buried in Tomb SS. According to the ten locally produced vessels, a LC IIA–B date or the 14th century BC is suggested.

## Chamber Tomb TT

BY RAINER FELDBACHER & PETER M. FISCHER

Chamber Tomb TT is located just to the north of Tombs RR and SS (plan and sections in *Figs. 9–11*). On the magnetometer map, this single-chamber tomb appears as a circular geophysical anomaly. A 4 × 5 m trench approximately 13.0 masl

was opened (see position in *Fig. 1*). At around 12.60 masl, the centrally placed entrance was discovered. The roughly circular outline of the uppermost part of the tomb has a diameter of approximately 2.75 m, and the almost square bottom of the tomb extends 3.5 m from west to east and 3.0 m from north to south, thus giving the tomb a “bottle neck” shape in profile. The entrance to the tomb is 1.30 m above the floor of the chamber.

### L201, L202, L204

The upper part of the tomb, L (Locus) 201, L202, and L204 extends from *c.* 12.60 masl to 11.80 masl (blue in *Fig. 9*). The yellowish-grey backfilled soil in the upper part contained numerous pieces of havara,<sup>10</sup> the local name of a surficial, soft, porous, white to buff, carbonaceous, clastic rock of Quaternary age that is widespread in Cyprus. The concentration of havara in the backfill made it possible to distinguish the tomb from the surrounding natural soil without havara.

Except for a broken wall bracket of fired clay (L201-1) and a piece of a lamp also from L201 in a small niche to the north, the backfilled soil of L201 and L202 did not contain any objects of relevance to the burials. There are a few mollusc shells and pieces of copper slag, but these items can be found

<sup>10</sup> E.g., Schirmer 1998.

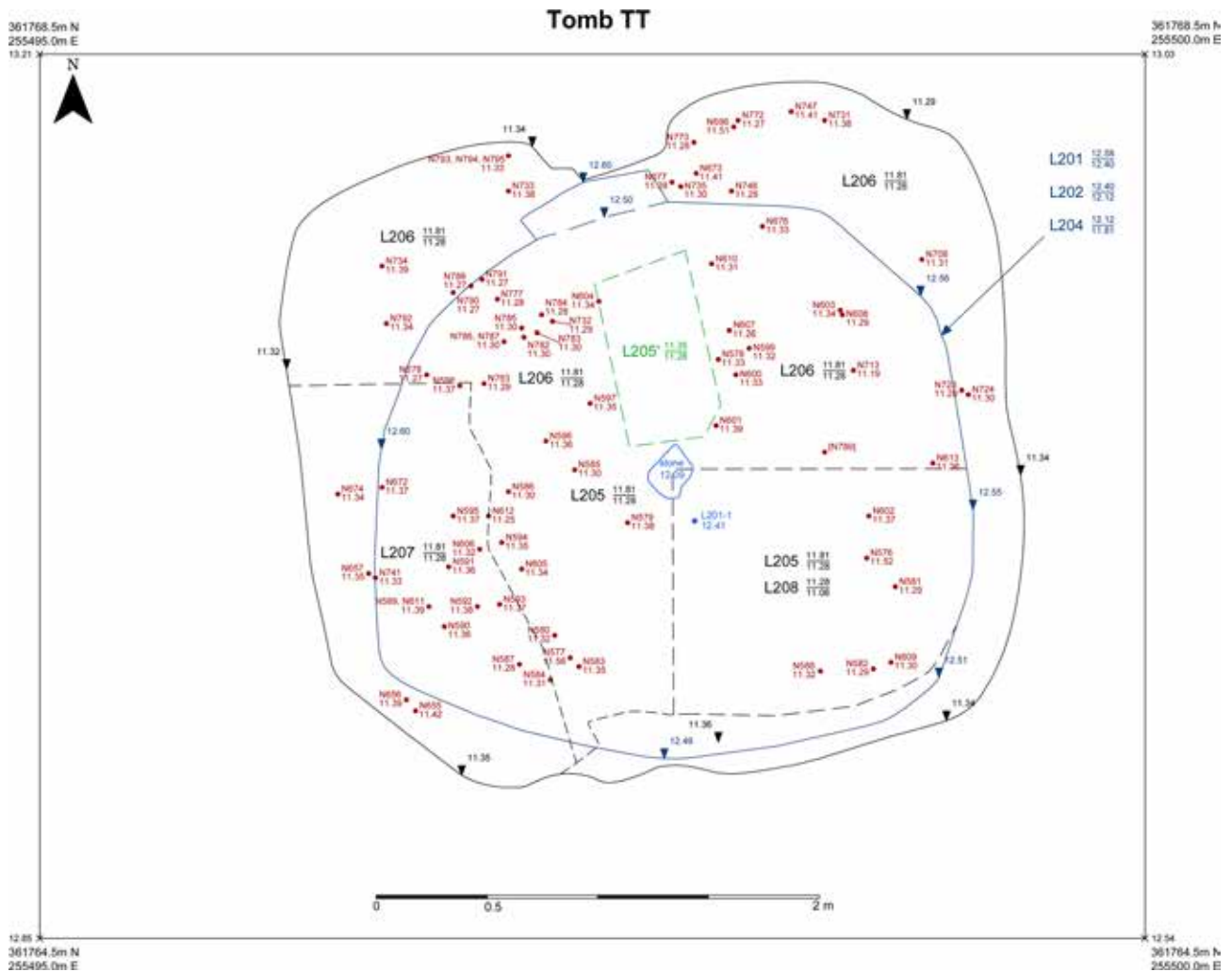


Fig. 9. Chamber Tomb TT: co-ordinates and heights of trench, loci, and finds (in red); upper part of tomb in blue; lower part in black; structure within tomb in green (by A. Papageorgiou and C. Sofokleous, modified by R. Feldbacher and P.M. Fischer).

everywhere in the ploughed soil of Area A. In the lower part of L204, White Slip II and Base-ring sherds appeared in the backfill which gradually became softer and changed colour to reddish-brown until quite a hard layer of clay appeared which covers numerous intact or complete vessels of fired clay. Below these finds are the skeletal remains of 25 (MNI) individuals (L205 directly below L204).<sup>11</sup>

#### L205, L206, L207, L208

The loci containing entombments and burial gifts, from *c.* 11.80 masl to the bottom of the tomb at *c.* 11.20 masl, were labelled L205, L206, and L207. These loci are on ap-

proximately the same level, where L205 encompasses the central and south-eastern parts of the tomb, L206 the northern and north-western, and L207 the western and south-western parts. The lower portion of the tomb widens gradually towards the floor which covers an area of 3.5 × 3.0 m. To locate the bottom level of the tomb, L208,<sup>12</sup> a *c.* 1 × 1 m test trench was dug through the bottom of L205. Only geological layers were exposed in this locus. The only structure in the tomb is a rectangular cut into a white chalky material, 0.7 × 0.4 m and 0.07 m deep (L205'; green in Fig. 9), which divides L206 into two portions. A concentration of finds was discovered to the west and east of this cut.

<sup>11</sup> See *Appendix 1*.

<sup>12</sup> Dashed black lines in the south-eastern part of tomb (see Fig. 9).

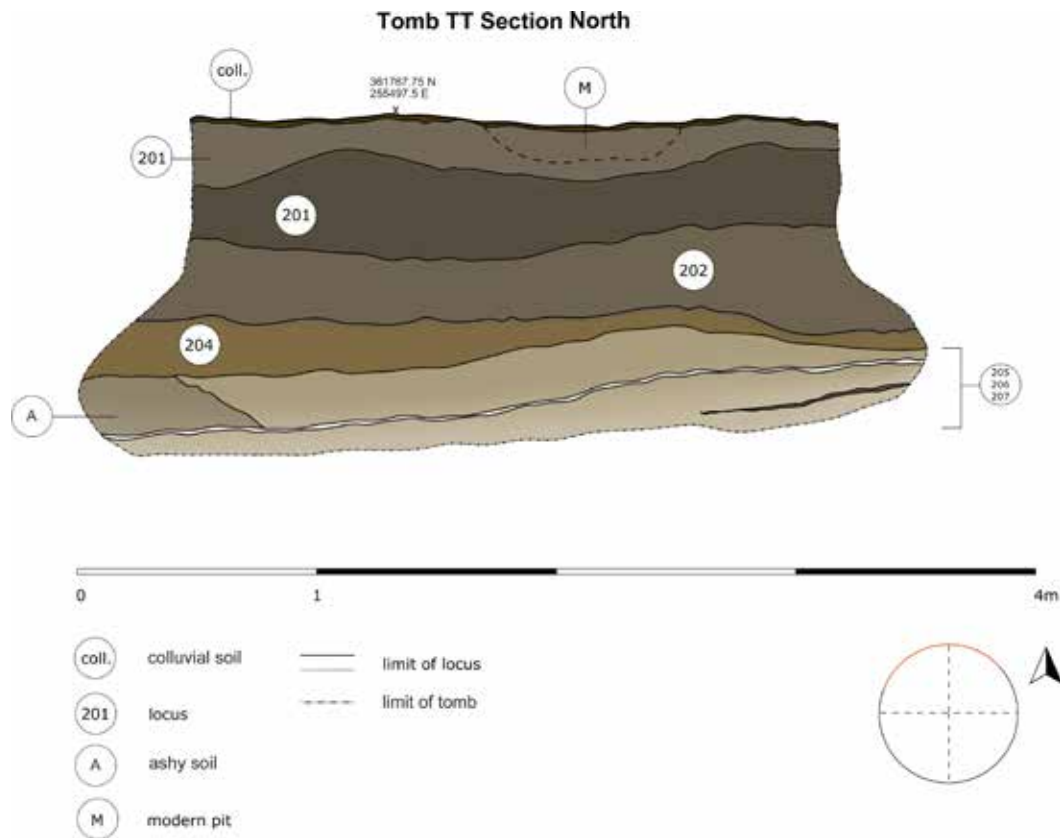


Fig. 10. Chamber Tomb TT: loci projected along the northern fill of the tomb (by M. Pelc).

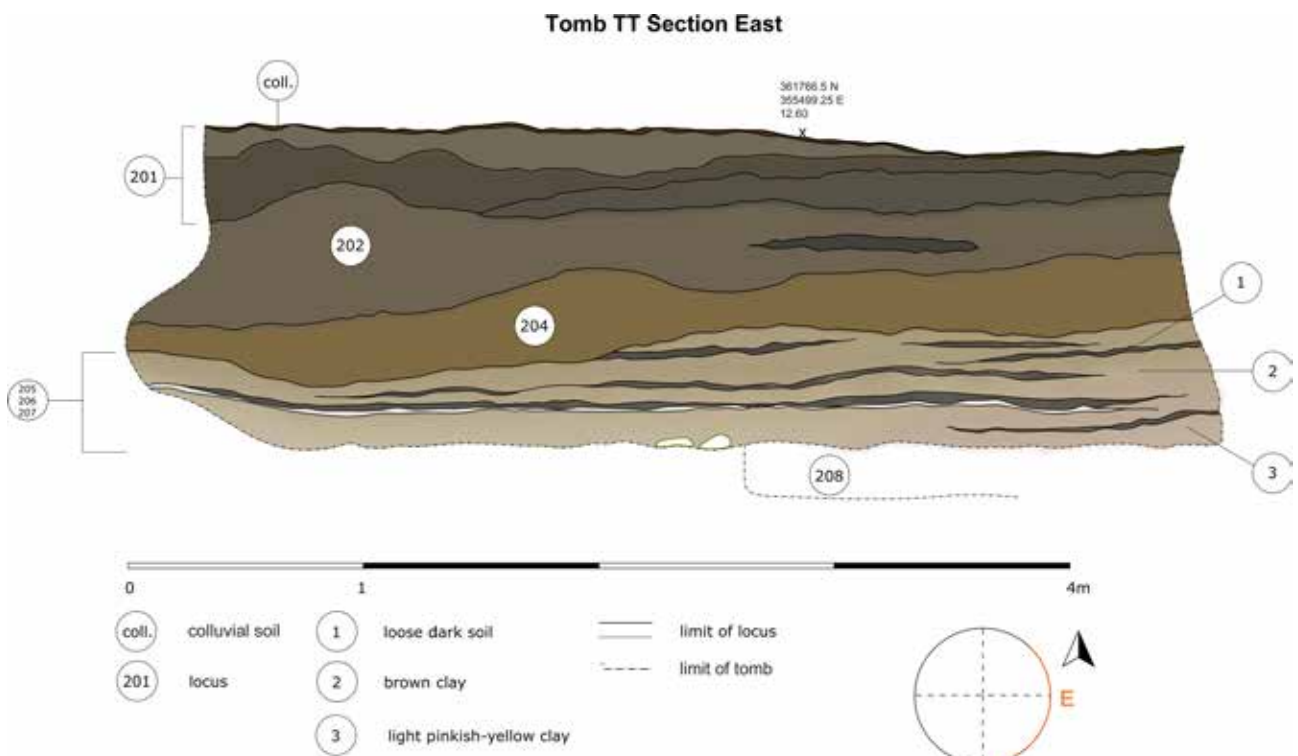


Fig. 11. Chamber Tomb TT: loci projected along the eastern fill of the tomb (by M. Pelc).

Table 5. Finds from Chamber Tomb TT arranged primarily according to loci and object types.

Find (N)	Locus	Material	Classification/Type	Shape/Object
N588	L205	bronze	bracelet	triple spiral
N605	L205	bronze	ring	double spiral
N592	L205	clay	Base-ring I	bowl
N580	L205	clay	Base-ring I	juglet
N609	L205	clay	Base-ring I	juglet
N577	L205	clay	Base-ring II	jug
N581	L205	clay	Base-ring II	jug
N583	L205	clay	Base-ring II	jug
N584	L205	clay	Base-ring II	jug
N587	L205	clay	Base-ring II	jug
N600	L205	clay	Base-ring II	jug
N601	L205	clay	Base-ring II	jug
N603	L205	clay	Base-ring II	jug
N607	L205	clay	Base-ring II	jug
N608	L205	clay	Base-ring II	jug
N593	L205	clay	Base-ring II	lentoid flask
N578	L205	clay	Base-ring II	undefined
N597	L205	clay	Bucchero	juglet
N591	L205	clay	Monochrome	jug
N611	L205	clay	Mycenaean	alabastron (straight sided)
N604	L205	clay	Mycenaean	juglet
N579	L205	clay	Mycenaean	piriform jar (medium)
N674	L205	clay	Mycenaean	small three-handled jar
N576	L205	clay	Plain White	jug
N582	L205	clay	Plain White	jug
N599	L205	clay	Plain White	jug
N590	L205	clay	Plain White	juglet
N585	L205	clay	White Slip II	bowl
N586	L205	clay	White Slip II	bowl
N594	L205	clay	White Slip II	bowl
N595	L205	clay	White Slip II	bowl
N596	L205	clay	White Slip II	bowl
N598	L205	clay	White Slip II	bowl
N602	L205	clay	White Slip II	bowl
N606	L205	clay	White Slip II	bowl
N610	L205	clay	White Slip II	bowl
N613	L205	clay	White Slip II	bowl
N657	L205	clay	White Slip II	bowl
N589	L205	clay	White Slip II	bowl
N789	L205	gold	raw material	piece of rod, cut
N678	L205	ivory	spindle whorl?	Flat conical
N612	L205	silver (?)	pendant/sheet (?)	-
N763	L206	bronze	balance weight	sphendonoid

Table 5 continued.

Find (N)	Locus	Material	Classification/Type	Shape/Object
N788	L206	bronze	balance weight	sphendonoid
N673	L206	bronze	bracelet	circular (small)
N735	L206	bronze	bracelet	circular with open ends
N708	L206	clay	Base-ring II	jug
N773	L206	clay	Base-ring II	juglet
N734	L206	clay	Mycenaean	piriform jar (medium)
N733	L206	clay	Plain White	bowl
N772	L206	clay	White Painted VI	feeding bottle
N676	L206	clay	White Shaved	juglet
N748	L206	clay	White Shaved	juglet
N677	L206	clay	White Slip II	bowl
N696	L206	clay	White Slip II	bowl
N786	L206	faience	bead	spherical
N731	L206	faience	“bead” (?)	dome-shaped
N793	L206	gold, carnelian, faience	beads from bracelet	spherical, elongated, cylindrical
N777	L206	haematite	balance weight	sphendonoid with flattened bottom
N791	L206	haematite	balance weight	sphendonoid, one flattened side
N785	L206	haematite	balance weight	sphendonoid
N787	L206	haematite	balance weight	sphendonoid
N783	L206	haematite	balance weight	sphendonoid (half)
N792	L206	ivory	distaff, part	rod
N747	L206	ivory	lid	lid
N794	L206	ivory/bone	scarab	scarab
N790	L206	limestone	balance weight	sphendonoid, two flattened sides
N795	L206	paste	beads (c. 20)	spherical/elongated, fluted
N732	L206	bone/ivory	scarab	scarab
N782	L206	glass/faience	scarab	scarab
N784	L206	silver	earring (part)	circular
N713	L206	silver	finger ring	circular
N723	L206	silver	ring	double spiral
N724	L206	silver	ring	double spiral
N656	L207	clay	Base-ring I	juglet
N672	L207	faience	2 beads	spherical/elongated, fluted
N655	L207	rock crystal	raw material (?)	hexagonal with pointed end
N741	L207	silver	ring	ring



Fig. 12. Chamber Tomb TT, selected Cypriot pottery including White Slip II bowl with human remains (N610) and Base-ring II lentoid flask in situ (N593, conservation impending. Photographs J. Ahola, L. Avial Chicharro and P.M. Fischer).



Fig. 13. Chamber Tomb TT, selected Mycenaean pottery and small finds (photographs J. Abola, L. Avial Chicharro and P.M. Fischer).



Fig. 14. Chamber Tomb TT, the scarabs (photographs P.M. Fischer).

### Burial gifts

Altogether, 78 objects were uncovered in this tomb (see *Table 5*; *Figs. 12–15*). The inhumations are associated with 47 ceramic vessels of which the vast majority were intact. The only imported pottery comprises five Mycenaean vessels. Cypriot pottery consists of 42 vessels of Base-ring I and II, Bucchero, Monochrome, Plain White, White Painted VI, White Shaved, and White Slip II (mature/normal). Other finds were of bronze, gold, silver, ivory, faience, haematite, and minerals. Several of them were parts of jewellery and others functioned as balance weights.

### The scarabs<sup>13</sup>

Fig. 14; see also *Appendix 2*.

#### N732

Scarab, bone or ivory,<sup>14</sup> 12 × 8 × 6 mm.

Base: a Ma'at-feather with a uraeus in front; both are hatched and facing to the right; below an *nb*-sign; borderline; scarabs with these three elements occur several times but always with the uraeus behind the Ma'at-feather;<sup>15</sup> a cryptographic reading of the name of Amun cannot be ruled out. Date: 18th Dynasty (*c.* 1400–1300 BC).

#### N782

Scarab, glass/faience,<sup>16</sup> green surface with brown colouring, heavily worn with deep cracks, although appropriately stored, it broke into pieces, 15 × 10 × 8 mm.

Base:<sup>17</sup> the upper part of the design shows in horizontal arrangement a lion striding to the right with one front paw lifted (the motif is indicated by those parts which are of brownish

colour); the rear is missing; in the lower section of the plinth, i.e., below the horizontal crack, a second element is discernible having roughly the shape of an elongated *nb*-sign; there are four main motifs showing a solitary lion striding (not seated or crouching) over an object; the latter may be the stylized hieroglyph *n* in the shape of a simple line or variants thereof which may also include a *mn*-sign; a human figure lying on the ground; the hieroglyph *nb* or a crocodile but the latter is most likely: the object below the crack is undoubtedly not linear which excludes the stylized *n*-line (there is also no *j*-hieroglyph in front of the lion, which is typical for this motif); it can be excluded that the lion is striding over a human figure as there are no discernible traces of limbs or of a head; an *nb*-hieroglyph may be considered but usually this combination shows an additional uraeus in front of the lion which is missing here; moreover the lifted paw of the lion suggests a gesture of domination over another being and not a *nb*-sign, such is the case when the lion is striding over a crocodile; the lion may even be depicted as placing its raised paw on the crocodile's head; in another representations the lion is stepping on the reptile's head; it should be noted that the brownish colour, which indicates the parts of the motif, extends on the right side above the horizontal crack below the suggested lifted paw, which may indicated remains of the crocodile's head; although not conclusive due to the worn state of the seal, but not an argument against but rather for the crocodile, is that the elongated object seems to be dissected which would corresponds to the manner in which the crocodile is often represented in the proposed motif; lastly, the slightly wavy-like shaped crack or suggested upper delimitation of the motif rather fits a crocodile than an *nb*-sign; due to the known motifs (irrelevant due to their shape are single representations of horned animals or a uraeus below a striding lion) and the process of elimination, the crocodile comes into question as the most probable motif in the lower section of the plinth.<sup>18</sup>

Date: Late MB IIB/LC I (Hyksos period, *c.* 17th century BC).

#### N794

Scarab, ivory/bone,<sup>19</sup> 14 × 10 × 8 mm.

Base: in a horizontal arrangement *Mn-hpr-r*, throne name of Thutmose III in an oval flanked by Ma'at-feathers with outward-pointing uraeus.<sup>20</sup>

<sup>13</sup> We are greatly indebted to Jürg Egler, University of Fribourg, Switzerland, who studied the scarabs. For parallels consult: Egler & Keel 2006; Hall 1913; Keel 1994; 1995; 1997; 2010a; 2010b; 2013; 2017; Murray *et al.* 1900; Tufnell 1953.

<sup>14</sup> According to the XRF analysis in *Appendix 2*.

<sup>15</sup> Identical to the present arrangement is only Keel 1997, Tell el-Ağul no. 232 from tomb 1057 of cemetery VI dated to LB IIB (1400–1300 BC).

<sup>16</sup> According to the XRF analysis in *Appendix 2*.

<sup>17</sup> Cf. the diverging results of the analyses of the scarab's base in *Appendix 2*. The poor state of preservation of the green scarab did not allow any information to be extracted on its carved decoration without a further

iconographic in-depth study of numerous related scarabs. This comparative study has been carried out by J. Egler.

<sup>18</sup> Keel 1995, § 541.

<sup>19</sup> According to the XRF analysis in *Appendix 2*.

<sup>20</sup> For the motif see Keel 1997, Tell el-Ağul no. 295; 2010b, Tell el-Far a-Süd nos. 646, 827; 2013, Tel Gamma no. 61 & Geser no. 357; Lachish in Tufnell 1953, pl. 43:3; 1958, pls. 37/38:283; Enkomi in Murray *et al.* 1900, 41, pl. 4:694 ("uncertain localisation" = Hall 1913, 153, no. 1563).

Date: 18th Dynasty (from Thutmose III–19th Dynasty; 1494–1186 BC).

### Discussion of Chamber Tomb TT

Based on the position of the magnetic anomaly, a 4 × 5 m trench was positioned around the centre of the anomaly. The subsequently discovered tomb appeared almost exactly in the centre of this trench. This demonstrates the accuracy of the co-ordinates of the magnetic anomalies which were recorded and mapped during the large-scale survey in 2017.

The layer of clay in L204 just below the soft backfill (L201, L202) seems to have had a shielding function. In the centre of this locus was a flat stone which might have served as the base for a (wooden?) pole to support a protecting roof when the tomb was opened again. This arrangement would explain the wall bracket (L201-1) and the part of a lamp in a niche in the northern compartment of the tomb which were used when the tomb was reopened.

Certain contexts demonstrate the intentional arrangement of bones belonging to previously interred generations. One example is the skeletal concentration labelled SK3 where specific anatomical elements seem to have been grouped (i.e., stacked ilia deriving from multiple different individuals). Another example is the commingled remains from the area designated as SK6&7 (*Fig. 16* and plan in *Fig. 40* in *Appendix 1*) which were delimited by a rectangular perimeter made of lower limb bones, primarily femora.

Considering the multitude of imports in other tombs that have been discovered by the current project, the scarcity of imported material, which is restricted to a few vessels of Mycenaean pottery, is noteworthy. Nevertheless, this may just indicate an early phase with fewer imports from the Mycenaean cultural sphere compared to the mass of Mycenaean vessels in LH IIIA2 (1350–1300 BC).

A piece of raw gold (N789, 3.42 g), which had been cut from a longer bar with the cut marks still visible, points to the local production of gold jewellery. There is, for instance, a mould of steatite from City Quarter 2 (CQ), Stratum 1 for casting a finger ring.<sup>21</sup> Jewellery from Chamber Tomb TT comprises a few beads of gold, faience, and carnelian, finger- and earrings of silver and bronze, and bracelets of bronze of which one in the shape of a triple spiral is quite substantial (60 g). Four objects are of ivory: a distaff (N792), a lid (N747), and two scarabs (N732 and N794).<sup>22</sup> There is also a piece of natural rock crystal which possibly represents a talisman.

Eight sphenonoid-shaped balance weights are of haematite, bronze, or stone (*Fig. 15* lower; *Table 6*). Only one of the haematite weights has a round section. Two of haematite (N787, N791) have ground-down sides, and another two of haematite have completely flattened bottoms (N777, N783) thus they appear as “half-weights”. The limestone weight (N790) has also a ground bottom.

*Figure 15* (upper) and *Table 7* show another collection of balance weights of haematite from Tomb LL at Hala Sultan Tekke, excavated in 2017.<sup>23</sup> Tomb LL is dated between 1450 and 1350 BC, or roughly LC IIA(–B). This shaft tomb contained nine sphenonoid-shaped balance weights of haematite together with a whetstone of hornblende (*Fig. 15* upper two rows). The whetstone seems to have been used to grind down only the pointed parts of the sphenonoids to their targeted masses which contrasts with the weights from Chamber Tomb TT, where all pointed ends were ground down but some of the weights also have flattened sides.

The masses of the weights from Tomb LL are in decreasing order (in g): 28.3, 19.5, 7.4, 5.6, 4.0, 2.9, 2.1, 1.8, and 1.0. We suggested then the following weight system in relation to a theoretical standard weight of 9.4 g:<sup>24</sup> 3× (standard), 2×, 4/5×, 3/5×, 2/5×, 1/3×, 1/5×, 1/5× and 1/9×. In the collection of balance weights from Tomb LL, the actual standard weight is missing but this weight can simply be achieved by using two lighter weights. Karl M. Petruso suggested somewhat different attributions to four of the weights:<sup>25</sup> 3×, 2×, 3/4×, –, –, 1/3×, –, –, –. No doubt, the precision of the equipment which was used to produce them was lowest at very low masses. Consequently, the error might have been relatively high for the lightest specimens.

It seems that the masses of the balance weights from these two tombs, which are approximately 150 m apart (see *Fig. 2* where Tomb LL is to the north-east of Chamber Tomb TT), cannot be compared, except for N788 of bronze and N144 of haematite, both at approximately 5.6 g. Whether these dissimilarities are dependent on chronological factors—Tomb LL is possibly somewhat older than Chamber Tomb TT—or other factors cannot be answered at present. Another difference is the choice of material for the balance weights which can be related to the rank of the inhumed individual(s). The manufacture of the haematite weights was certainly more time-consuming (“expensive”) than those of limestone or bronze. Nevertheless,

<sup>21</sup> Fischer & Bürge 2018b, 473–476, 482, fig. 4.34:8.

<sup>22</sup> N732 might be produced of bone but N794 seems to be ivory. In any case, they are of an organic material according the XRF analyses.

<sup>23</sup> Fischer & Bürge 2018a, 53–62.

<sup>24</sup> The proportions are slightly corrected compared to the results in Fischer & Bürge 2018a. According to Petruso 1984, the standard weight in the Eastern Mediterranean has a mass of c. 9.4 g. See also the same standard weight used by Pulak 2000 on the balance weights from the Late Bronze Age shipwreck at Uluburun.

<sup>25</sup> Pers. comm., 30 June 2017.



Fig. 15. Balance weights. Upper: Tomb LL, weights of haematite and whetstone of hornblende for grinding down the weights to the desired mass. Lower: Chamber Tomb TT, weights of haematite, bronze, and limestone (photographs P.M. Fischer).

Table 6. Balance weights from Chamber Tomb TT, Locus 206.

Find	Material	Shape/Object	Weight (g)
N790	limestone	sphendonoid, two flattened sides	2.59
N763	bronze	sphendonoid	3.38
N777	haematite	sphendonoid with flattened bottom	4.73
N783	haematite	sphendonoid (half)	5.00
N788	bronze	sphendonoid	5.59
N791	haematite	sphendonoid, one flattened side	8.42
N787	haematite	sphendonoid	13.40
N785	haematite	sphendonoid	20.58

Table 7. Balance weights from Chamber Tomb LL, Locus 99.

Find	Material	Shape/Object	Weight (g)
N149	haematite	sphendonoid	1.0
N148	haematite	sphendonoid	1.8
N146	haematite	sphendonoid	2.1
N147	haematite	sphendonoid	2.9
N145	haematite	sphendonoid	4.0
N144	haematite	sphendonoid	5.6
N143	haematite	sphendonoid	7.4
N142	haematite	sphendonoid	19.5
N141	haematite	sphendonoid	28.3

when comparing the “wealth” of these tombs,<sup>26</sup> there are only minor differences: imports from Tomb LL comprise a Late Minoan II/IIIA piriform jar with excellently painted motifs of

birds and plants, an Anatolian Red Lustrous Wheel-made bottle, and a Levantine juglet together with a diadem of gold but no other imports, whereas Chamber Tomb TT contained four Mycenaean imports and several scarabs. These differences may not represent differing ranks of the buried individuals but simply show the owners’ predilection for certain objects.

The five Mycenaean vessels from Chamber Tomb TT are best placed in Late Helladic IIIA(2) which corresponds roughly to the 14th century BC, possibly the second half of this century. This is also supported or at least not contradicted by several vessels of Base-ring I and II, and White Slip II mature/normal style. Mature White Slip I which was produced during the reign of Thutmosis III is missing.<sup>27</sup> There are some White Slip II bowls which show early traits. The Base-ring I and II wares do not contribute to narrow the use of the tomb: Base-ring I has quite a long life span, and it overlaps that of Base-ring II which also has been demonstrated by numerous contexts at Hala Sultan Tekke (see ‘Discussion’ below and Fig. 38).<sup>28</sup>

The green-coloured scarab N782, which dates to the 17th century BC, must be considered as an heirloom since no other finds would allow such an early date for the use of the tomb. In general, scarabs are poor chronological indicators and provide only a *terminus post quem* in relation to the reign of a specific pharaoh if they have a royal cartouche. An example is the scarab with the cartouche of Thutmosis III (N794 in Fig. 14) from Chamber Tomb TT. Scarabs with the cartouche of this mighty pharaoh were very popular and produced and circulated

<sup>26</sup> Observe that our perception of wealth may differ from that in the Bronze Age.

<sup>27</sup> Cf. Fischer 2003; Fischer & Bürge 2017.

<sup>28</sup> Åström 1972, 700–701.



*Fig. 16. Chamber Tomb TT with assembled skeletal remains in the north-western part; inset: detail of finger rings of silver in situ. (photographs P.M. Fischer).*

ed in a vast area long after his reign (1494–1440 BC).<sup>29</sup> One has also to consider that scarabs which were produced during or shortly after his reign could have been kept as heirlooms for a considerable period.

Considering the arrangements of the skeletal remains of 25 (MNI) (e.g., *Fig. 16*) and the nature and arrangements of the burial gifts, it seems that the tomb was used for quite a short period. Since bones of previously buried individuals were arranged, two phases of entombments are the lowest possible number, but it may be extended to include a third.

All evidence considered together, a date for the tomb just after 1350 BC is proposed. This corresponds to LC II(A–)B or LH IIIA(2).

## Chamber Tomb UU

BY PETER M. FISCHER

In May 2022, approximately 100 m to the north-west of Chamber Tomb TT, the author observed a concentration of sherds and human bones which had been exposed by farming. The co-ordinates of this area in a recently harvested field were linked to the magnetometer map, where an unusually large magnetic anomaly of approximately 10 × 10 m could be discerned. To enclose the entire magnetic anomaly, a 20 × 15 m-large area was fenced off just to north of a dirt road (see

the area in *Fig. 17*). Due to the restricted remaining time in the field, a test trench of not more than 4 × 4 m was opened.

Fragments of human bones were present in the colluvial soil. As soon as the colluvial soil (0.15–0.20 m from the present surface) was removed, it became clear that the test trench did not cover the entire area occupied by the tomb as was suggested by the size of the magnetic anomaly.

### L300, L301, L302, L303, L303', L304'

After removing the colluvial soil, the upper part of the tomb was divided in six loci mainly for practical reasons (*Fig. 18*). These loci are on approximately the same level: L300, L301, and L302 in the central-western part of the tomb, L303' in the western, and L303/L304 in the eastern part. L304' includes the upper contexts in this area, and L304 (see below) the lower contexts. Most significant for these contexts are numerous disarticulated human bones intermingled with complete and in many cases intact objects. The 17 finds comprise pottery of Base-ring I and II, Plain White, Red Lustrous Wheel-made, White Shaved, and White Slip II, as well as a finger ring of bronze and pieces of copper slag (*Table 8*).

### L304, L305

A stone layer appeared *c.* 0.2 m below the surface in the northern part of the trench, and in the south-western corner is a large, 10 cm-thick stone slab. To the south of the stone layer are L304 and L305, which do not differ stratigraphically ex-

<sup>29</sup> Fischer 2013, 540, fig. 466:2.



Fig. 17. Drone photograph of Tomb UU (later part of season; photograph P.M. Fischer).

Table 8. Finds from Tomb UU arranged primarily according to loci and types of objects.

Find (N)	Locus	Material	Classification/Type	Shape/Object
N628	L301	bronze	ring	circular, ends overlap
N615	L301	clay	Red Lustrous Wheel-made	spindle bottle
N616	L301	clay	Red Lustrous Wheel-made	spindle bottle
N625	L301	copper	slag	-
N636	L302	clay	Base-ring	jug
N635	L302	clay	Base-ring II	juglet
N619	L303	clay	Base-ring	juglet
N620	L303	clay	Base-ring I	juglet
N626	L303	clay	Base-ring I	juglet
N622	L303	clay	Base-ring II	bowl
N621	L303	clay	Plain White	bowl
N617	L303	clay	Red Lustrous Wheel-made	flask
N627	L303	clay	White Shaved	juglet
N614	L303	clay	White Slip II	bowl
N618	L303	clay	White Slip II	bowl (large)
N623	L304'	clay	Plain White	bowl
N624	L304'	clay	Base-ring I	juglet
N765	L304	calcite	base of N764	"tazza"
N712	L304	clay	Base-ring	bowl
N717	L304	clay	Base-ring	juglet
N759	L304	clay	Base-ring	bowl
N760	L304	clay	Base-ring I	bowl
N761	L304	clay	Base-ring I	bowl
N706	L304	clay	Base-ring I	jug
N705	L304	clay	Base-ring I	krater
N738	L304	clay	Base-ring II	bowl

Table 8 continued.

Find (N)	Locus	Material	Classification/Type	Shape/Object
N740	L304	gold	diadem	elongated sheet
N709	L304	clay	Late Minoan (?)	juglet
N762	L304	clay	Mycenaean	piriform jar
N756	L304	clay	Plain White	bowl
N739	L304	clay	Red Lustrous Wheel-made	spindle bottle
N764	L304	calcite	small handleless cup	"tazza"
N707	L304	gold; faience	two beads	elongated; flat/globular
N746	L304	clay	White Shaved	juglet
N743	L304	clay	White Slip II	bowl
N745	L304	clay	White Slip II	bowl
N757	L304	clay	White Slip II	bowl
N770	L304	clay	White Slip II	bowl
N693	L305	calcite	calcite	juglet
N730	L305	silicate mineral	asbestos	sample
N722	L305	bronze/silver	balance weight (?)	bovine head (?)
N668	L305	clay	Base-ring	bowl
N758	L305	clay	Base-ring	bowl
N661	L305	clay	Base-ring I	bowl
N647	L305	clay	Base-ring I	jug
N694	L305	clay	Base-ring I	jug
N718	L305	clay	Base-ring I	jug
N780	L305	clay	Base-ring I	jug
N691	L305	clay	Base-ring I	juglet
N692	L305	clay	Base-ring I	juglet
N720	L305	clay	Base-ring I	juglet
N702	L305	clay	Base-ring I	krater

Table 8 continued.

Find (N)	Locus	Material	Classification/ Type	Shape/Object
N648	L305	clay	Base-ring I	tankard
N667	L305	clay	Base-ring I	tankard
N639	L305	clay	Base-ring II	jug
N644	L305	clay	Base-ring II	jug
N645	L305	clay	Base-ring II	jug
N646	L305	clay	Base-ring II	jug
N652	L305	clay	Base-ring II	jug
N681	L305	clay	Base-ring II	jug
N682	L305	clay	Base-ring II	jug
N688	L305	clay	Base-ring II	jug
N716	L305	clay	Base-ring II	tripod vessel
N775	L305	gold	bead	profiled, hollow
N698	L305	ivory	cosmetic box	duck-shaped
N642	L305	clay	Canaanite	jar
N675	L305	clay	Canaanite	jar
N715	L305	clay	Canaanite	jar
N781	L305	ivory	distaff	pomegranate pommel
N771	L305	ivory	distaff, part?	pointed
N699	L305	calcite	lid of N693	lid
N631	L305	clay	Late Minoan	one-handed goblet
N753	L305	clay	Monochrome	bowl
N703	L305	clay	Mycenaean	piriform jar
N651	L305	clay	Mycenaean	piriform jar (medium)
N653	L305	clay	Mycenaean	piriform jar (medium)
N650	L305	clay	Mycenaean	piriform jar (small)
N659	L305	clay	Mycenaean	piriform jar (small)
N721	L305	clay	Mycenaean	shallow cup
N660	L305	clay	Mycenaean	three-handled jar
N649	L305	clay	Plain White	bowl
N663	L305	clay	Plain White	bowl
N669	L305	clay	Plain White	bowl
N684	L305	clay	Plain White	bowl
N689	L305	clay	Plain White	bowl
N700	L305	clay	Plain White	bowl
N701	L305	clay	Plain White	bowl
N710	L305	clay	Plain White	bowl
N711	L305	clay	Plain White	bowl
N727	L305	clay	Plain White	bowl
N736	L305	clay	Plain White	bowl
N737	L305	clay	Plain White	bowl
N751	L305	clay	Plain White	bowl
N752	L305	clay	Plain White	bowl
N767	L305	clay	Plain White	bowl
N768	L305	clay	Plain White	bowl

Table 8 continued.

Find (N)	Locus	Material	Classification/ Type	Shape/Object
N629	L305	clay	Plain White	jug
N638	L305	clay	Plain White	jug
N719	L305	clay	Plain White	jug
N729	L305	clay	Plain White	jug
N704	L305	clay	Plain White	krater
N695	L305	clay	Red Slip	juglet
N643	L305	clay	Red Lustrous Wheel-made	spindle bottle
N662	L305	clay	Red Lustrous Wheel-made	spindle bottle
N755	L305	clay	Red Lustrous Wheel-made	spindle bottle
N769	L305	clay	Red Lustrous Wheel-made	spindle bottle
N630	L305	clay	Red Lustrous Wheel-made	spindle bottle
N714	L305	shell	shell	shell with perforation
N774	L305	ivory	spindle; whorl	pointed; conical
N725	L305	stone	whetstone	rectangular
N665	L305	clay	White Shaved	juglet
N671	L305	clay	White Shaved	juglet
N690	L305	clay	White Shaved	juglet
N632	L305	clay	White Slip II	bowl
N637	L305	clay	White Slip II	bowl
N640	L305	clay	White Slip II	bowl
N641	L305	clay	White Slip II	bowl
N654	L305	clay	White Slip II	bowl
N658	L305	clay	White Slip II	bowl
N664	L305	clay	White Slip II	bowl
N666	L305	clay	White Slip II	bowl
N670	L305	clay	White Slip II	bowl
N679	L305	clay	White Slip II	bowl
N680	L305	clay	White Slip II	bowl
N683	L305	clay	White Slip II	bowl
N685	L305	clay	White Slip II	bowl
N686	L305	clay	White Slip II	bowl
N687	L305	clay	White Slip II	bowl
N726	L305	clay	White Slip II	bowl
N728	L305	clay	White Slip II	bowl
N754	L305	clay	White Slip II	bowl
N779	L305	clay	White Slip II	bowl
N633	L305	clay	White Slip II	tankard
N634	L305	clay	White Slip II	tankard
N749	L307	clay	Mycenaean	piriform jar
N742	L307	clay	Mycenaean	piriform jar (small)
N750	L308	clay	Base-ring II	jug
N766	L308	clay	Bucchero	juglet
N776	L308	clay	Mycenaean	piriform jar
N778	L308	clay	Mycenaean	piriform jar

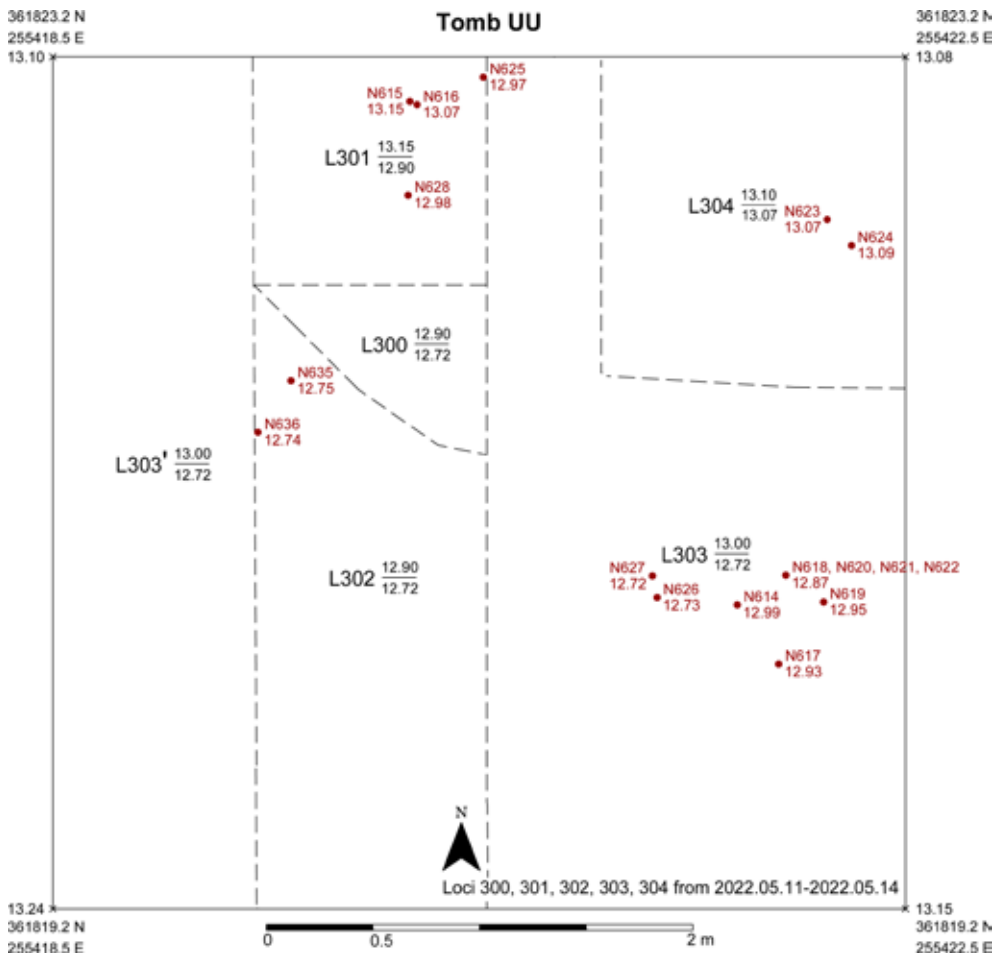


Fig. 18. Tomb UU with L300, L301, L302, L303, L303', L304 (by A. Papageorgiou and C. Sofokleous, modified by P.M. Fischer and J. Tracz).

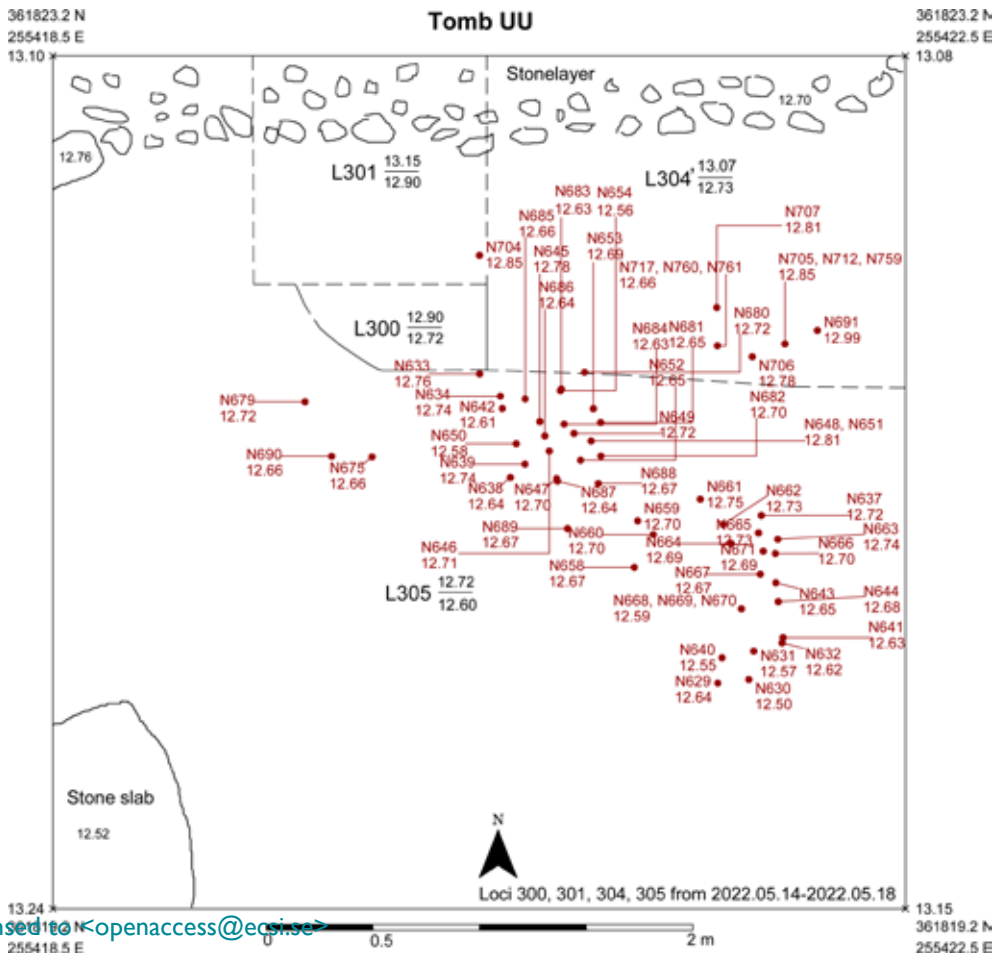


Fig. 19. Tomb UU with L300, L301, L304, L305 (by A. Papageorgiou and C. Sofokleous, modified by P.M. Fischer and J. Tracz).

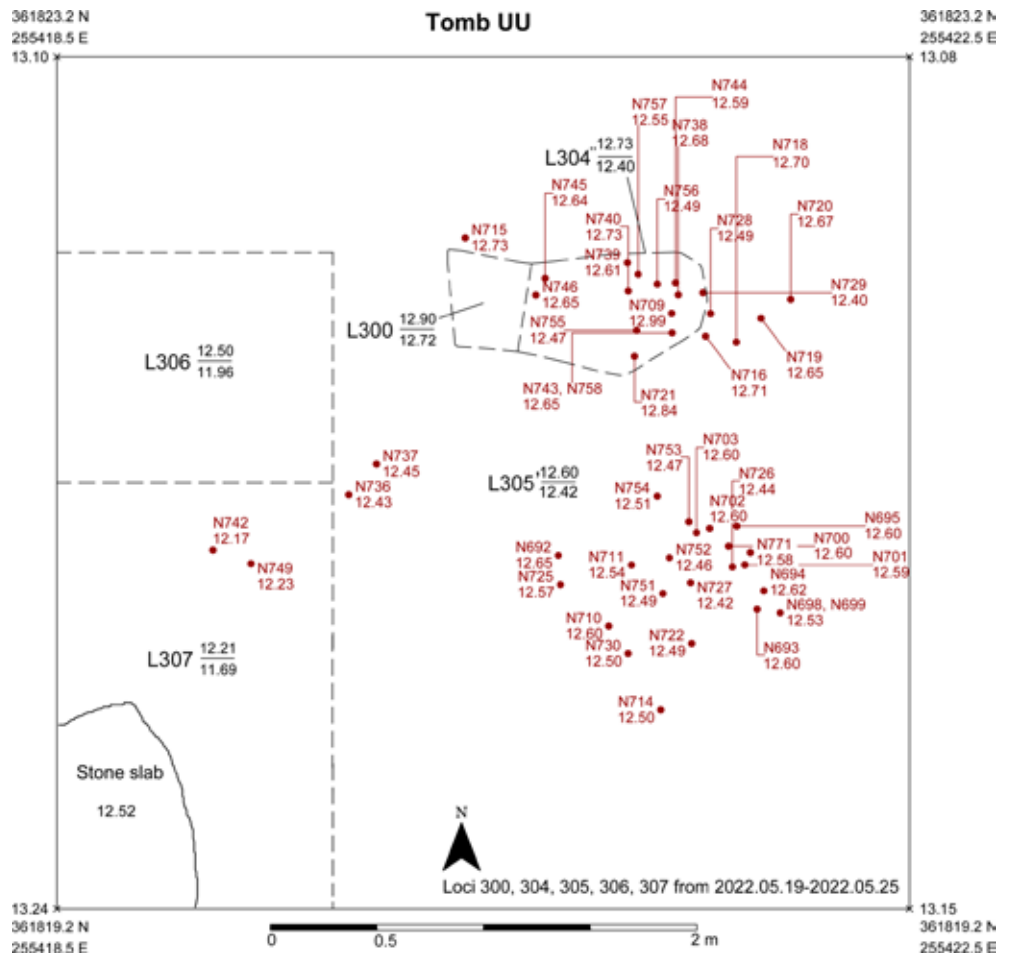


Fig. 20. Tomb UU with L300, L304, L305, L306, L307 (by A. Papageorgiou and C. Sofokleous, modified by P.M. Fischer and J. Tracz).

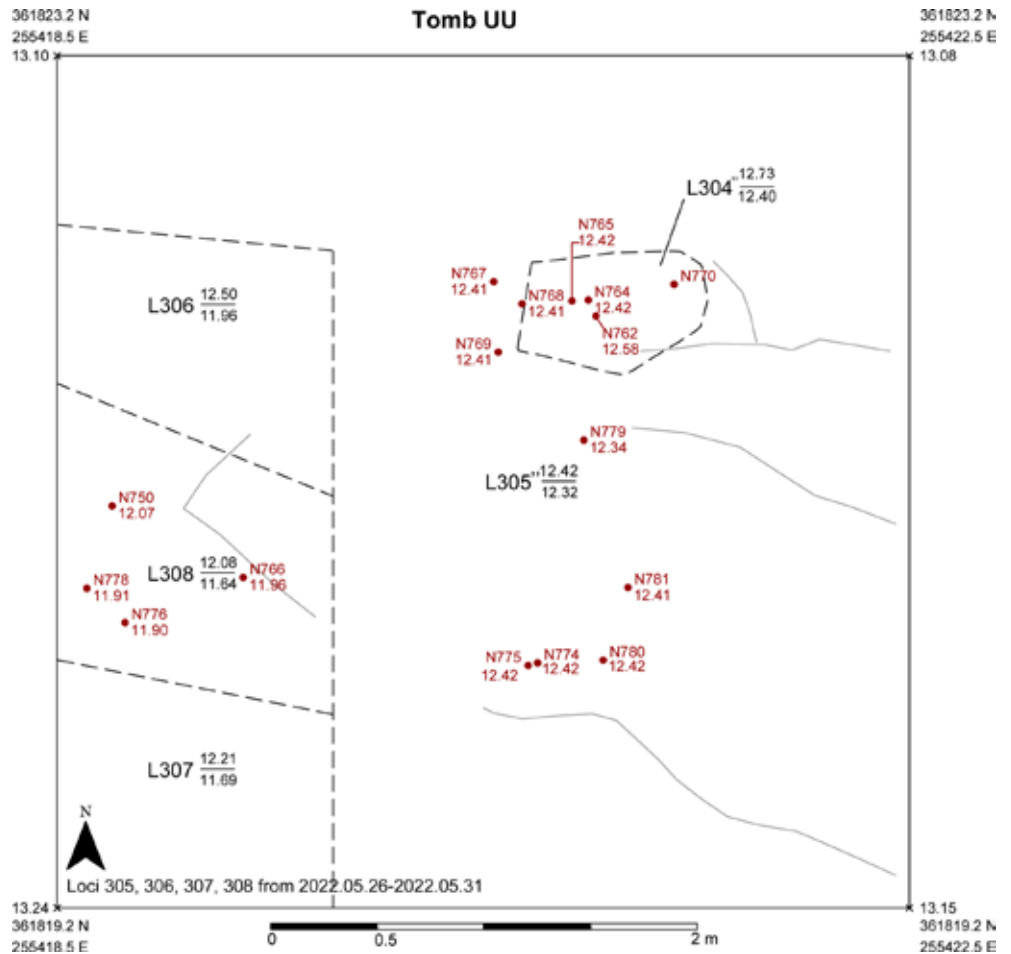


Fig. 21. Tomb UU with L304, L305, L306, L307, L308 at the end of the season (by A. Papageorgiou and C. Sofokleous, modified by P.M. Fischer and J. Tracz).

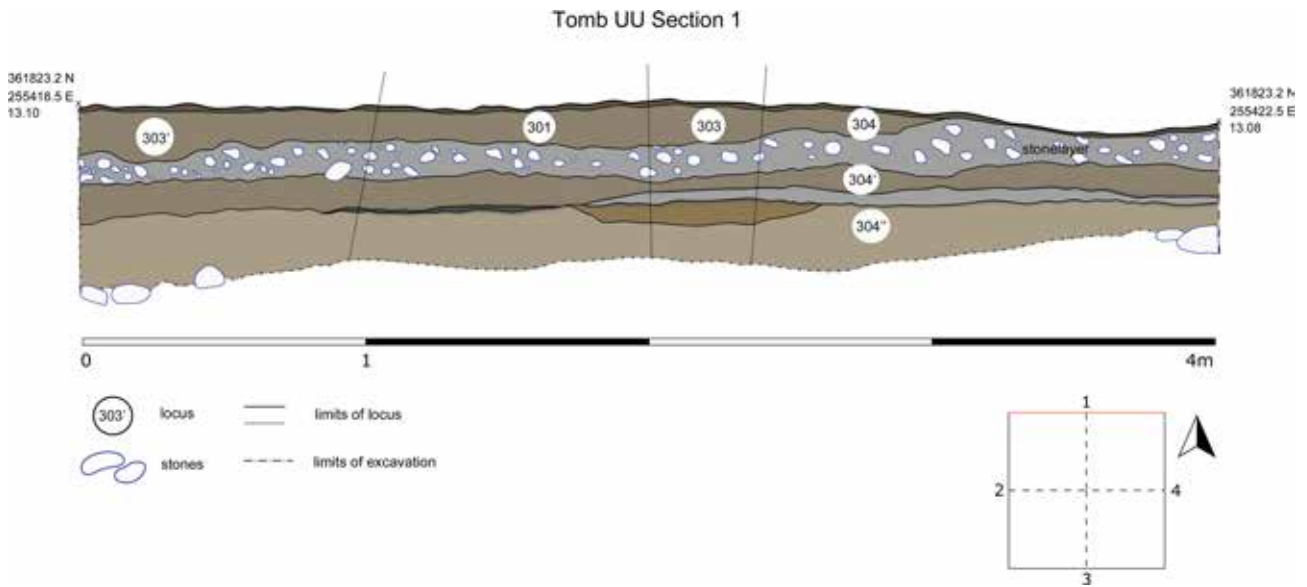


Fig. 22. Tomb UU. Section 1, North (by M. Plec, modified by P.M. Fischer).

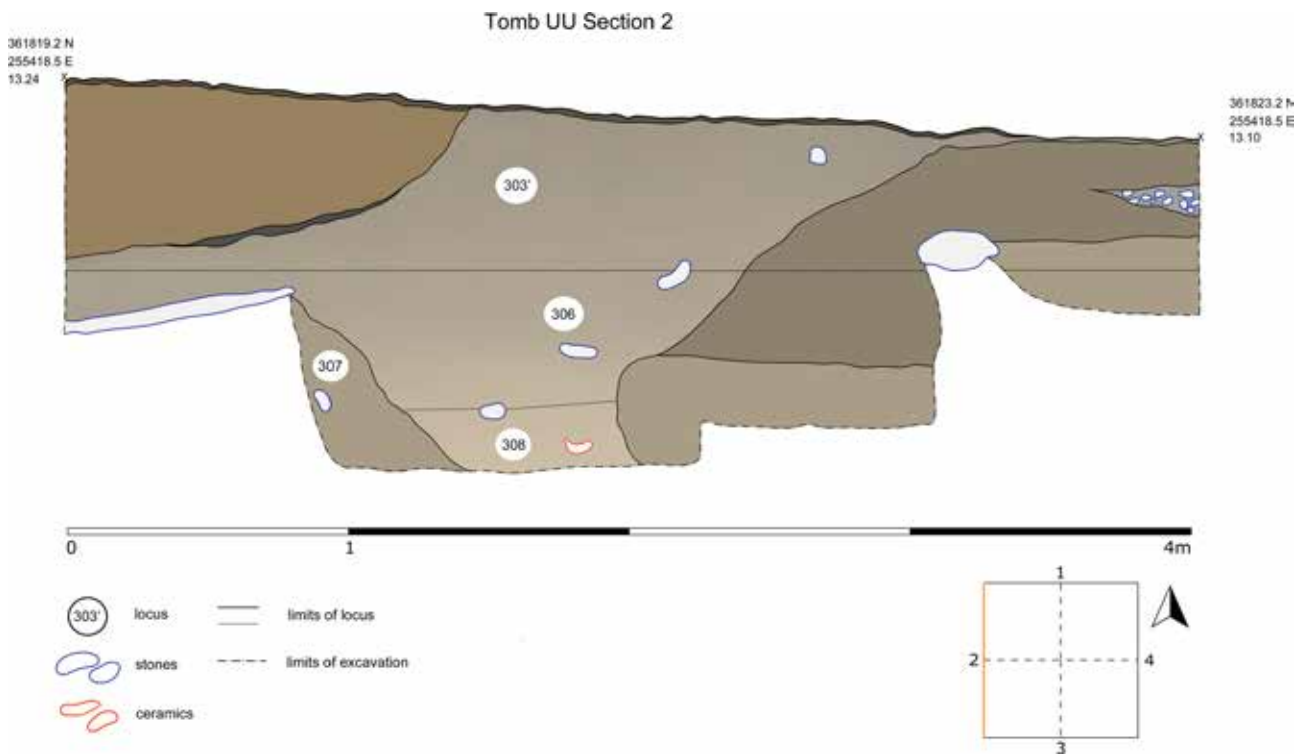


Fig. 23. Tomb UU. Section 2, West (by M. Plec, modified by P.M. Fischer).

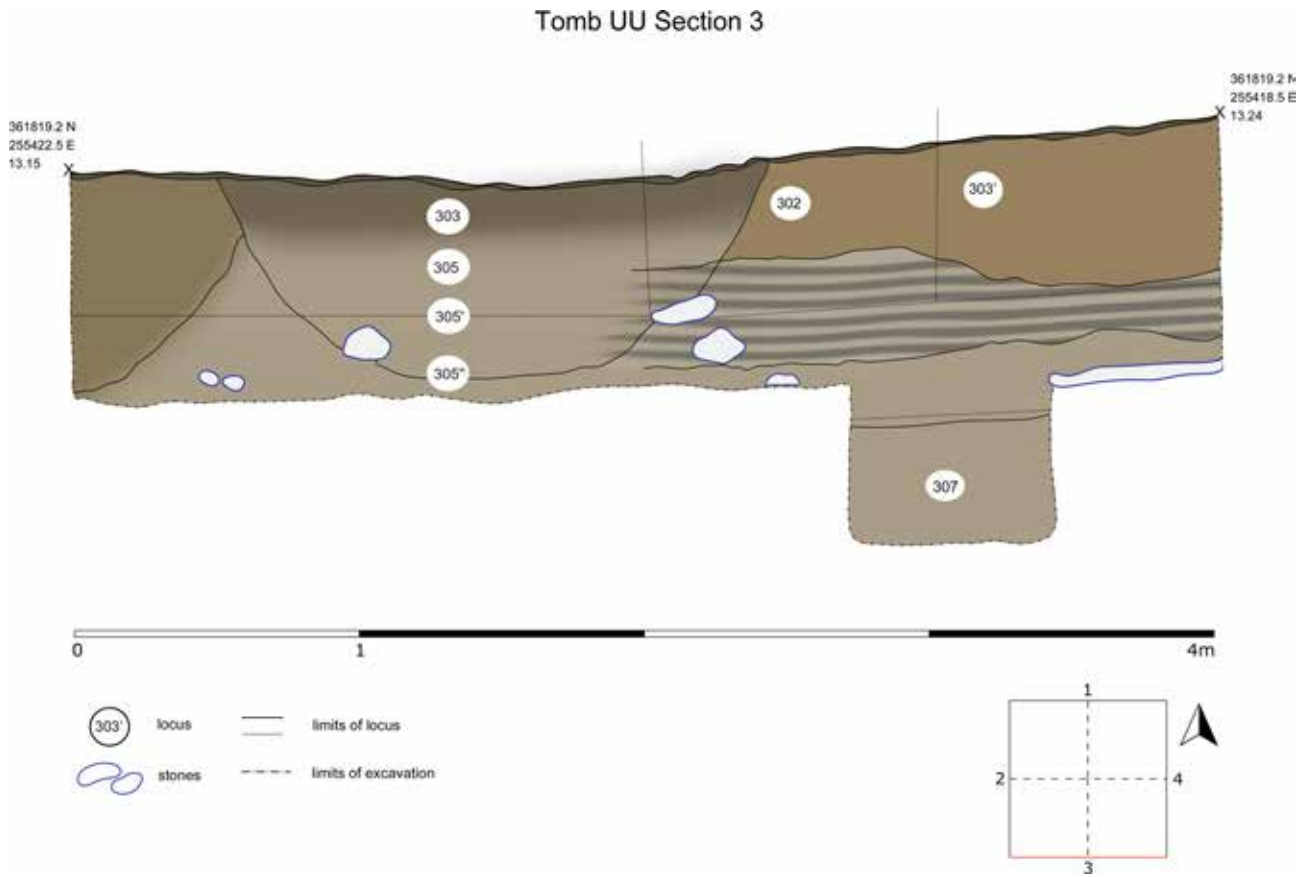


Fig. 24. Tomb UU. Section 3, South (by M. Plec, modified by P.M. Fischer).

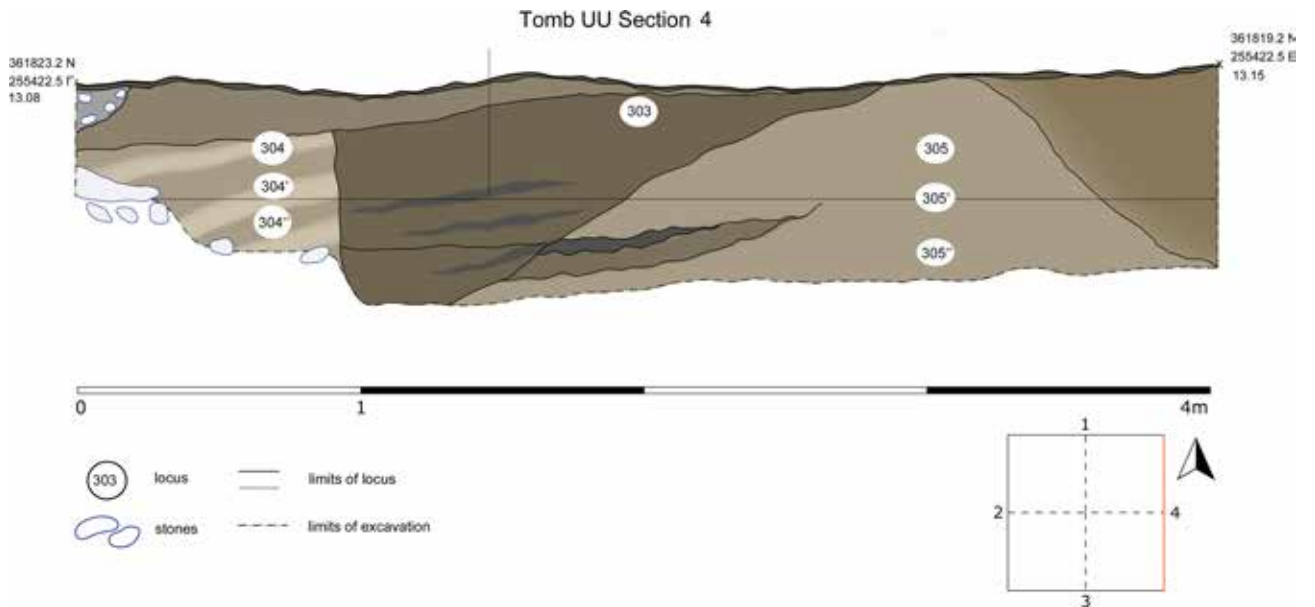


Fig. 25. Tomb UU. Section 4, East (by M. Plec, modified by P.M. Fischer).



Fig. 26. Tomb UU. Cypriot pottery (photographs P.M. Fischer).



Fig. 27. Tomb UU. Cypriot pottery (photographs P.M. Fischer).



Fig. 28. Tomb UU. Cypriot pottery (photographs P.M. Fischer).

cept for their location in the horizontal plane: L304 is mainly in the north-eastern and L305 in the south-eastern part of the trench (Figs. 18–25). In these loci, a few (partially) articulated skeletons were found together with 117 objects, the majority being intact or at least complete. The preliminary osteological investigation points to a minimum of 19 individuals (four nonadults and 15 adults) based on the dentition (see *Appendix 1*). There are patterns of bone placement, including the stacking of os coxae (cf. Chamber Tomb TT where the long bones were arranged before a subsequent interment). The semi-articulated skeletons were all disarticulated below the rib cage.

The 140 objects so far retrieved from Tomb UU are described in *Table 8*. The Cypriot ceramics comprise Base-ring I

and II, Bucchero, and Monochrome (Figs. 26–28), White Shaved, White Slip II (Figs. 28, 29), Plain White, and Red Slip. Imported wares are Canaanite jars, Late Helladic, and Late Minoan pottery (Fig. 30), and Anatolian Red Lustrous Wheel-made wares (Fig. 31 upper). Other finds are of Egyptian calcite (Figs. 31, 32), ivory (Fig. 33), gold (Figs. 34, 35), silver, bronze, faience, and various minerals. There are also mollusc shells and animal bones.

Most of the locally produced vessels belong to the standard repertoire of ceramics from the second half of the Late Cypriot period. Nevertheless, there are rare vessels, not only at Hala Sultan Tekke but also in Cyprus in general: two tankards of Base-ring I (N648; N667 in Fig. 28), and two tankards of White Slip II (N633, N634; both in Fig. 28) which appear to



Fig. 29. Tomb UU. Cypriot pottery (photographs J. Ahola and P.M. Fischer).

belong to the early production of White Slip II. A Base-ring II amphoriskos-like vessel with three legs attached to the ring base shows a rare decoration (N716; Fig. 26).

The six Mycenaean and one Mycenaean-type (most likely Cypriot-produced) vessels comprise medium and small piri-form jars, and a shallow cup with a vertical handle (Fig. 30).<sup>30</sup> A one-handled goblet (N631) and a juglet (N709) are preliminarily classified as Late Minoan (both Fig. 30 lowest row). There are nine vessels of Red Lustrous Wheel-made ware: eight are spindle bottles and one is a flask (Fig. 31). The various Canaanite jars were imported from the Levant.

Two vessels of white calcite from L305 are the first of their kind from the current project (Figs. 31, 32). The calcite juglet (N693) with lid (N699), and next to it a *tazza* also of calcite manufactured of two parts (N764 bowl and N765 base), are Egyptian imports of superior quality. The calcite juglet was located near a large complete Base-ring I jug (Fig. 32 left). The overall shape of the juglet resembles very much that of the Base-ring I jug (see 'Discussion'). From the same context as the calcite juglet comes an ivory cosmetic box in the shape of a duck, also the first discovered at Hala Sultan Tekke (N698;

<sup>30</sup> Concerning N660, see 'Discussion'.



Fig. 30. Late Helladic (N650, N659, N653, N651, N742, N721), Mycenaean-type (N660), and two Late Minoan (N631, N709) pottery vessels (photographs J. Abola, L. Avial Chicharro and P.M. Fischer).

Fig. 32 right).<sup>31</sup> Another object of ivory is a distaff: it is complete with the rod (N771) and the head shaped as a pome-

granate (N781; Fig. 33). In L304, among commingled skeletal remains including crania was a diadem of gold (N740), and an elongated fluted gold bead (N707; Figs. 34, 35). Another

<sup>31</sup> The head of a duck cut from hippopotamus ivory comes from an unknown tomb at Enkomi (British Museum no. 1897,0401.1379). [https://www.britishmuseum.org/collection/object/G\\_1897-0401-1379](https://www.britishmuseum.org/collection/object/G_1897-0401-1379)

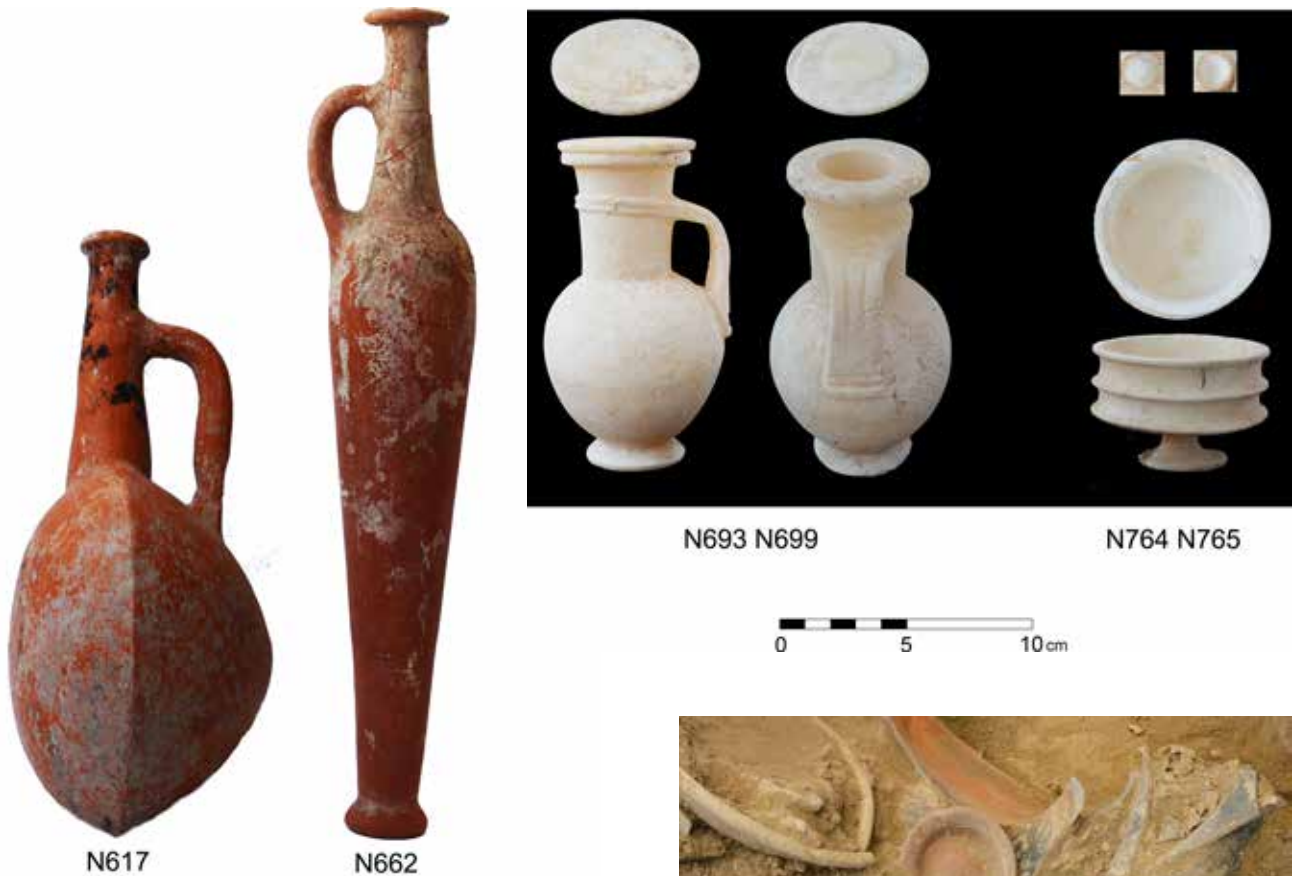


Fig. 31. Tomb UU. Left: Anatolian pottery; right: Egyptian calcite vessels (photographs P.M. Fischer).

bead of gold came from L305 (N775; Fig. 35). Among the minerals were pieces of asbestos (Fig. 36).<sup>32</sup>

### L306, L307, L308

At the end of the season, a 0.75 m-wide test trench was opened along the western margins of the square (Figs. 20, 21, 23, 24). L306 to the north is devoid of any finds. In L307, approximately 0.2 m below the lowest finds of L305”, were two Mycenaean piriform jars which do not differ from those in L305”. In L308 the so-far lowest area of the tomb was reached at 11.64 masl, *viz. c.* 1.6 m below the surface (“3” in Fig. 37). L308 contained a Base-ring II jug, a Bucchero juglet, and two Mycenaean piriform jars which also can be compared with corresponding vessels in L304, L305, and L307.



Fig. 32. Tomb UU. Calcite juglet with lid, duck-shaped ivory box, and Base-ring I jug in situ (photograph P.M. Fischer).

<sup>32</sup> According to the fibrous appearance supported by XRF (analyses conducted by S. Hermon and his team at the Cyprus Institute).



Fig. 33. Tomb UU. Distaff of ivory (photograph P.M. Fischer).



Fig. 34. Tomb UU. Diadem of gold in situ (photograph P.M. Fischer).

## DISCUSSION OF TOMB UU

The conclusions and hypotheses presented here must be considered preliminary and may change during the continued exposure of this incompletely excavated tomb.

It seems that the stone layer to the north represents the northern margins of the tomb (“1” in Fig. 37). The function of the worked large stone slab in the south-eastern corner is not yet clear (“2” in Fig. 37). The shape and size are paralleled in Tomb RR.<sup>33</sup>

The remains of *c.* 19 individuals together with 140 objects were recovered. In consideration of the large number of skeletons and finds, the remaining 0.4 m of tomb material—as measured from the lowest finds in L305” (Fig. 37) to the uppermost finds in the so-far lowest context of L308 in the western test trench (“3” in Fig. 37)—will certainly contain more material and further information. In addition, the lowest level of L308 has not yet been reached.

It is interesting to note a 3–4 m wide “stripe” of skeletons and finds in L305” extending from the south-east to the north-west (lines in Fig. 21; see also Figs. 18–20). This observation can be interpreted in different ways: 1. an oblong chamber; 2. one chamber of a multi-chamber tomb where the other(s) are possibly to the south-east of the 4 × 4 m trench; and

<sup>33</sup> Fischer & Bürge 2020, 92, fig. 22.

3. a possible dromos leading to a chamber to the south-east. In addition to the superficial disturbances by the plough, it had initially been suggested that the disarticulated skeletons could be explained by attempts to loot the tomb. There are some indications of a “large pit” in the eastern section (Fig. 25), but this “pit” may just represent traces of the original tomb with backfill. The finds provide another counterargument against the theory that the tomb has been exposed to looters: most of them are intact or complete and several valuable objects are among them.

As previously mentioned, much of the locally produced pottery belongs to the standard repertoire of the LC IIA–B period. Quite a few find contexts in Tomb UU imply that the production of Base-ring I and II coincides (see e.g., Fig. 38). This has previously been observed both in the city and in other mortuary contexts. A new shape is a Base-ring II bowl with three stump legs decorated with an unusual pattern (N716; Fig. 26). Vessels used in cultic activities have previously been recorded in tomb contexts (e.g., the exclusive rhyton N330 from Tomb SS).<sup>34</sup> The Base-ring II bowl from Tomb UU might also have had a cultic function.

The Mycenaean piriform jars mostly fit the LH IIIA2 repertoire. Two small Mycenaean-type three-handled jars (N659 and N660; Fig. 30 upper row, second and fourth from left) are most likely of local production, possibly corresponding to Mycenaean-produced counterparts from LH IIIA1–2.<sup>35</sup> Two vessels, a one-handed goblet (N631) and a juglet (N709), are classified as Late Minoan (both Fig. 30 lowest row).<sup>36</sup>

Among the jewellery is a gold diadem (Figs. 34, 35) which has parallels in Tomb LL<sup>37</sup> and RR,<sup>38</sup> both excavated during the current project. The Egyptian juglet of calcite with a lid, which imitates Base-ring I, was produced from the period of Hatshepsut and Thutmose III, i.e., the 15th century BC. Maybe just by chance, our juglet was found next to a Base-ring I jug which represents the Cypriot original of the diminished Egyptian imitation. The *tazza* is a genuine Egyptian product and consists of two separately manufactured parts that were found close together. The original assumption that the two parts were glued together, for instance, with a resin seems to be contradicted by two observations: one is that there are no traces of a resin (but maybe lost when used); the second is wear, both on the knob-like part of the base of the bowl and the concavity on the upper part of the stem, thus the parts fit with high precision. Maybe, this arrangement was

<sup>34</sup> Fischer & Bürge 2022, 41.

<sup>35</sup> Cf. Graziadio 2017.

<sup>36</sup> Petrography and neutron activation analysis (NAA) are planned.

<sup>37</sup> Fischer & Bürge 2018a, 58, fig. 25:12.

<sup>38</sup> Fischer & Bürge 2022, 27, fig. 10: N512. A similar diadem but with incised decoration was found in Tomb X, see Fischer & Bürge 2017, 178, fig. 12:6.

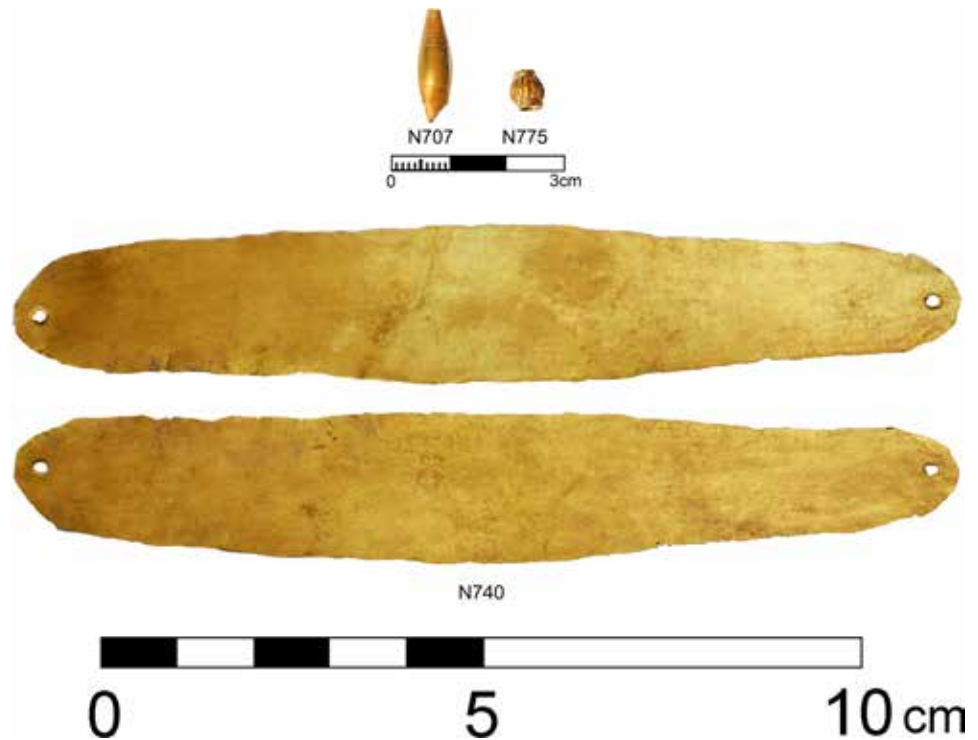


Fig. 35. Tomb UU. Finds of gold (photographs P.M. Fischer).

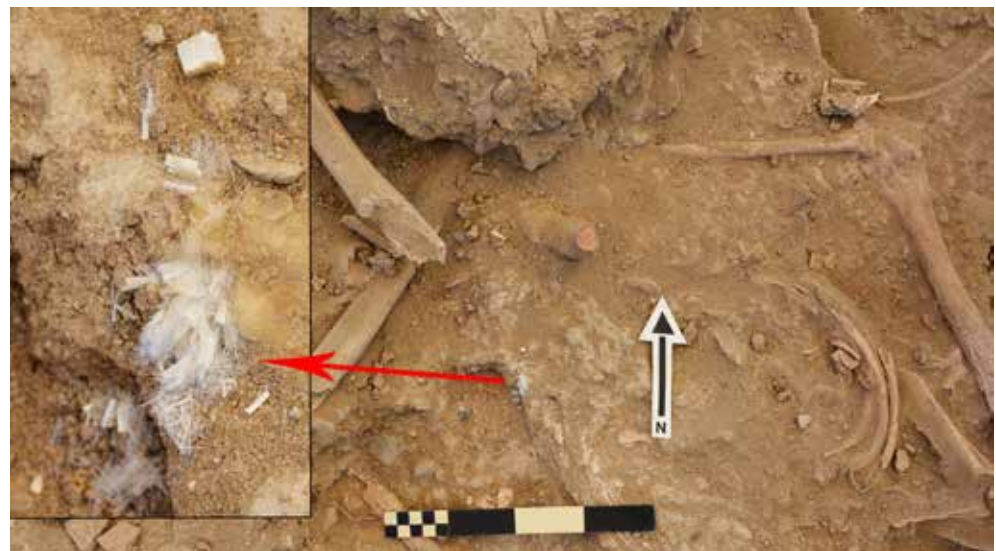


Fig. 36. Tomb UU. Pieces of asbestos (photographs P.M. Fischer).

deliberately done in order to be able to remove the bowl, fill it with the desired stuff and put it back again without moving the stem. In addition, it was certainly easier to get access to unevenly distributed contents just by rotating the bowl and not the entire vessel. In Egypt, the calcite vessels of the kind found in Tomb UU are normally restricted to tombs of the Egyptian élite.<sup>39</sup>

<sup>39</sup> Höflmayer 2012.

From the same context as the calcite vessels comes an Egyptian-manufactured ivory cosmetic box in the shape of a duck. The box was once covered by a rotatable lid which was attached to the container with a sort of “mushroom”-shaped rivet of ivory (still preserved).

According to the Mycenaean pottery, the uppermost burial layers can securely be dated to the 14th century BC (LC II [A–]B or LH IIIA[2]), and more precisely around or just after 1350 BC. This date is not contradicted by the locally pro-



Fig. 37. Orthophotograph of Tomb UU at the end of the spring 2022 season. 1. stone layer (northern limits?); 2. stone slab; 3. test trench; and L305'' lowest part of the regular excavations (drone photograph P.M. Fischer).

duced pottery, the Anatolian-imported Red Lustrous Wheel-made vessels, and the Egyptian imports.

## Summary and further research

The preliminary results of the 2022 fieldwork in the Late Bronze Age cemetery of the harbour city of Hala Sultan Tekke have shed further light on the interregional connections and the mortuary practices of the city's élite. Although already recognized in previous seasons, it should once more be emphasized that the tombs are in an extramural area, in contrast to the more common location of burials inside the settled area in the Late Cypriot period.<sup>40</sup> The latter is found in urban centres such as Enkomi *Ayios Iakovos*, Morphou *Toumba tou Skourou*,

Alassa, Kalavassos *Ayios Dimitrios*, and Kition.<sup>41</sup> Nevertheless, there is also evidence of intramural burials at Hala Sultan Tekke in Areas 8, 23, and CQ2.<sup>42</sup> The presence of an extramural cemetery, which is common in many parts of the Eastern Mediterranean, supports the impression of the intercultural character of the city's populations.

A characteristic feature of Late Cypriot mortuary practice is the use of tombs over generations, which has again been demonstrated by the contexts of Tombs TT and UU.<sup>43</sup> The tombs were reopened, body parts were moved and removed, and some skeletal remains and tomb gifts were re-arranged before new individuals were entombed (cf. Tombs X and LL).<sup>44</sup> The custom of secondary burials could be demonstrated in Pit Tomb L198, which was dug into the floor of the large

<sup>40</sup> For a recent and nuanced discussion on spatial dimensions of Late Cypriot burials see Webb 2018; see also Bürge 2021.

<sup>41</sup> See summary in Keswani 2004, 86–88.

<sup>42</sup> Fischer 1980, 16–18; Åström 1983; Niklasson 1983; Fischer & Bürge 2018a, 124, 129–134.

<sup>43</sup> Keswani 2004, 84–144.

<sup>44</sup> Fischer & Bürge 2017, 165, 169–195; 2018b, 53–58.

Tomb SS. Incomplete skeletons were moved from somewhere else and buried in the pit together with numerous tomb gifts. It seems likely that the builders of Tomb SS came across a previous burial. Due to respect for previously entombed generations, the contents of this tomb were (incompletely) reburied in the pit.

There are no skeletal remains in Offering Pit SS-S. Most of the vessels of this probable offering pit have quite small dimensions thus suggesting offerings for a child which likely had been interred in the adjacent Tomb SS, where several child burials could be recorded. According to the ten locally produced vessels, a LC IIA–B date or the 14th century BC is suggested.

The tombs which are mentioned in this report are Tombs X (single-chamber tomb), LL (rectangular shaft tomb), RR (double-chamber tomb, 8-shaped), SS (large single-chamber tomb of pentagonal shape), L198 (pit tomb), TT (circular single-chamber tomb), and UU (chamber tomb). All of them were used by the élite of the city judging by the luxurious burial gifts, of which many were imported. They include objects of gold, silver, bronze, ivory, faience, and various precious stones. There were also scarabs and numerous cylinder seals (though the latter group was not in the tombs excavated in 2022).

Summarizing the chronology of the listed tombs: they were used from the 16th century BC to *c.* 1200 BC, *viz.* LC IB to LC IIC. The earliest phase of the city's occupation is not yet represented in the material from the cemetery. The majority of the locally produced and imported objects can be dated to *c.* 1450–1300 BC which obviously represents the heyday of the city and corresponds to LC IIA(–B) to LC II (A–)B. Entombments without any tomb gifts, save for a few personal belongings, are represented by Tombs A,<sup>45</sup> and Z9 from LC IIIA or the first half of the 12th century BC.<sup>46</sup> The individuals from these tombs were buried in redundant wells.

Ongoing and future research include palaeoparasitological, micromorphological, archaeobotanical, and archaeozoological studies. In addition, bone (in specific *ossa petrosae*) and dental samples were collected for aDNA, Sr-isotope,



Fig. 38. Tomb UU. Context with Base-ring I and II (photograph P.M. Fischer).

and heavy metal analyses, and numerous vessels were sampled for organic residue analyses to study ritual consumption practices.<sup>47</sup>

PETER M. FISCHER  
Department of Historical Studies  
University of Gothenburg  
Contact: Dörjeskärgatan 37  
421 60 Västra Frölunda, Sweden  
peter@fischerarchaeology.se

TERESA BÜRGE  
Department of Historical Studies  
University of Gothenburg  
Box 200  
405 20 Gothenburg, Sweden

Institute of Archaeological Sciences  
University of Bern, Switzerland  
Austrian Archaeological Institute  
Austrian Academy of Sciences  
teresa.buerge@oeaw.ac.at

<sup>45</sup> Fischer & Bürge 2015, 41–44.

<sup>46</sup> Fischer & Bürge 2018b, 50, 60.

<sup>47</sup> This is part of a postdoctoral project on ritual deposition funded by an APART-GSK Fellowship of the Austrian Academy of Sciences awarded to Teresa Bürge.

## Appendix I. Human remains from Hala Sultan Tekke: Pit Tomb L198, Tomb SS, Chamber Tomb TT, and Tomb UU

BY KIRSI O. LORENTZ, BIANCA CASA, NATALIE M. BRANCA, YUKO MIYAUCHI, SILA KAYALP & MARIA NECTARIA ANTONIOU<sup>48</sup>

### INTRODUCTION

Human remains were recovered in 2021 and 2022 from Pit Tomb L198 (excavation completed), Chamber Tomb TT (excavation completed), and Chamber Tomb UU (excavation to be continued 2023). The following subsections outline the results of the macroscopic, metric, and contextual analyses of these remains, as well as an additional summary of Tomb SS human remains and mortuary programme. It should be noted that the comprehensive and definitive analyses of these remains in their site and tomb context will require the previously excavated human remains to be considered together with those that will presumably be excavated during forthcoming field campaigns.

### HUMAN REMAINS FROM PIT TOMB L198

Pit Tomb L198 was partially exposed during the 2021 excavation season and protected. It contained disarticulated human skeletal remains and mortuary artefacts, possibly relating to or predating the earliest interments in Tomb SS. The disarticulated state of human skeletal remains recovered from Pit Tomb L198 indicates secondary deposition.

The human skeletal remains recovered from Pit Tomb L198 are of relatively poor preservation status, including fragmented and incomplete skeletal elements. Bones from all areas of the body are represented, including crania, dentitions, vertebrae, *ossa coxae*, long bones, and smaller bones such as carpals, tarsals, and phalanges. The disarticulated human skeletal remains in the pit were stratigraphically separate

<sup>48</sup> Affiliation for all authors: The Cyprus Institute, Konstantinou Kavafi 20, 2121 Aglantzia, Nicosia, Cyprus. The authors acknowledge the financial support of the *Face to Face: Meet an Ancient Cypriot (FF-MAC)* project, which is co-financed by the European Regional Development Fund and the Republic of Cyprus through the Research and Innovation Foundation (grant no. INTEGRATED/0609/29; PI: KL). Further, the authors acknowledge the financial support of the *BioMERA: Platform for Biosciences and Human Health in Cyprus—MicroCT and Synchrotron Radiation Enabled Analyses* project, which is co-financed by the European Regional Development Fund and the Republic of Cyprus through the Research and Innovation Foundation (grant no. INFRASTRUCTURES/1216/09; PI: KL).

from the disarticulated human remains lining the perimeter of Tomb SS. No disarticulated remains were found in the loci overlying the L198 pit (L197, L150). The disarticulated remains were contained fully within the pit and its edges.<sup>49</sup> This contextual information is not inconsistent with the hypothesis that Pit Tomb L198 was an open feature in Tomb SS at the time of disarticulation of the original interments. The presence of mortuary artefacts may point to intentionality as to the placement of the skeletal elements into the pit. The following sub-sections detail the human remains recovered from Pit Tomb L198.

### MNI

The minimum number of individuals for Pit Tomb L198 is six, based on dental remains. MNI is a count of the most numerous skeletal element or tooth.<sup>50</sup>

### Age at death

The estimation of age at death was based on the morphology of the auricular surface of the ileum<sup>51</sup> and fusion of the iliac crest.<sup>52</sup> Three disarticulated ilia (two adult from the left, and one nonadult) could be used for age at death estimation, with age estimates of 30–34 years, 40–44 years, and <14–18 years (nonadult).

### Sex

Sexually dimorphic features of the pelvic bones and crania were assessed using the sex estimation guidelines of Jane E. Buikstra and Douglas H. Ubelaker.<sup>53</sup> Crania were used as they were the most frequent element present, though it should be noted that the pelvis is the most reliable skeletal element for estimation of sex. Two crania were complete enough for sex estimation, with L198\_Cran\_A consistent with a male sex estimate, and L198\_Cran\_B with a female sex estimate.

### Stature

The absence of intact larger long bones, metacarpals, or metatarsals preclude stature estimation for any individuals represented by the commingled remains from Pit Tomb L198.

<sup>49</sup> cf. Fischer & Bürge 2022, 37, 39.

<sup>50</sup> Bello & Andrews 2006; Robb 2016; Lorentz *et al.* 2021a.

<sup>51</sup> Lovejoy *et al.* 1985.

<sup>52</sup> Schaefer *et al.* 2009.

<sup>53</sup> Buikstra & Ubelaker 1994.

Table 9. Nonmetric traits present on dental remains from Pit Tomb L198 within Tomb SS.

Nonmetric trait		Permanent/Deciduous	Upper/ Lower	Tooth type	Side	Number of teeth with the trait	Locus num- ber
Carabelli's trait		Permanent	Upper	M1	right	1	L198
					left	2	L198; L182
		Permanent	Upper	M2	left	1	L198
Shovelling		Permanent	Upper	I1	left	1	L198
Supernumerary cusps	Metaconule	Permanent	Upper	M3	left	1	L198
		Permanent	Upper	M2	left	1	L198
	Entoconulid	Permanent	Lower	M1	left	2	L198
					right	1	L198

### Dental remains

In total, 59 permanent (22 maxillary and 37 mandibular) teeth and no deciduous teeth were recovered from Pit Tomb L198.

Dental pathologies present include linear enamel hypoplasia, dental caries, and dental calculus. Only one tooth, a lower left canine, displays linear enamel hypoplasia, associated with health-related stress at the time of dental development.<sup>54</sup> One medium-sized lesion of dental caries was noted at the cemento-enamel junction (CEJ) on the mesial aspect of an upper right third molar. Calculus was observed on 23% of the commingled teeth recovered from Pit Tomb L198, in either mild or moderate amounts. Dental nonmetric traits observed among the commingled loose teeth are Carabelli's trait, shovelling, and supernumerary cusps (Table 9).

### Skeletal pathologies

No skeletal pathologies were observed on the skeletal remains recovered from Pit Tomb L198.

### Summary of Pit Tomb L198 human remains

Pit Tomb L198 commingled remains present an MNI of 6, including a male and female. The estimation of age at death, where possible, indicates an adolescent, and two middle adults.

### HUMAN REMAINS FROM TOMB SS

Tomb SS was thoroughly investigated in 2020 and 2021. In 2022, only "cleaning-up" was carried out, *viz.* the complete exposure of the floor of this large tomb. The pattern of interment in Tomb SS overall includes both primary inhumations (presumably subsequently moved to the perimeters of the

tomb, after decomposition), and disarticulated and partially articulated remains. Following secondary disposal some skeletal elements remained in articulation (e.g., L139, SK1), or regions of skeletons remained in partial articulation. Disarticulated remains were subsequently overlaid by primary inhumations, represented by fully articulated skeletons.<sup>55</sup> These articulated skeletons were concentrated around the perimeters of the tomb chamber, leaving a space in the central area of the tomb devoid of human remains. This central area contained a concentration of broken pottery and intentionally deposited intact vessels which were suggested to represent the remains of feasting inside the tomb. These features were recovered during the 2020 and 2021 seasons.<sup>56</sup>

### MNI

The MNI in Tomb SS including articulated and disarticulated remains is ten, which is based on dental remains. When accounting for age-at-death differences, and in specific, the additional articulated and partially articulated foetal and infant individuals without dental remains, the total Tomb SS MNI is eleven.<sup>57</sup>

### Age at death

Tomb SS included one foetal individual, two infants, two children, two adolescents, and four adults.<sup>58</sup>

<sup>54</sup> Lorentz *et al.* 2019; 2021c.

<sup>55</sup> Fischer & Bürge 2022, 55; 2021, 132.

<sup>56</sup> Fischer & Bürge 2021, 110; 2022, 29.

<sup>57</sup> Fischer & Bürge 2022, 55–58; 2021, 131–134.

<sup>58</sup> Fischer & Bürge 2022, 55–58.

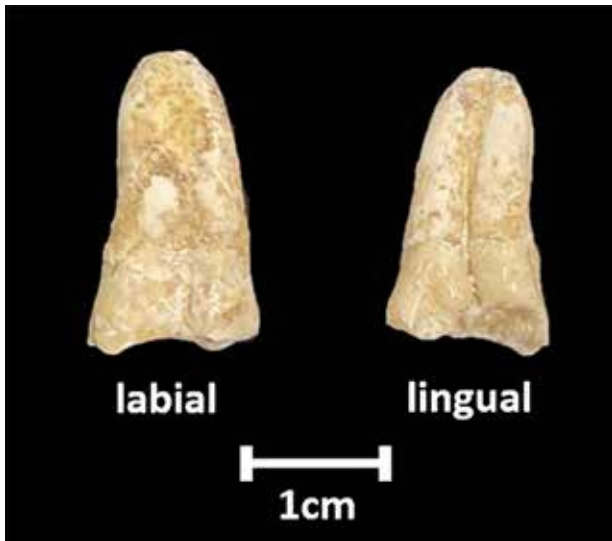


Fig. 39. Fused left first and second maxillary incisors (labial and lingual view) from L181, Tomb SS (Image by N. M. Branca).

### Sex

In total, sex could be estimated for seven discrete individuals within Tomb SS. These seven include two females, three probable females, one male, and one probable male.<sup>59</sup>

### Dental remains

Aside from the previously reported dentitions associated with the articulated individuals (SKs 1–11) recovered from Tomb SS, a total of 40 loose permanent teeth (20 maxillary and 20 mandibular), as well as nine loose deciduous teeth (all maxillary) were recovered from commingled contexts within the Tomb chamber of Tomb SS, not considering Pit Tomb L198.<sup>60</sup>

Dental nonmetric traits observed among the commingled loose teeth from Tomb SS are Carabelli's trait, shovelling, and supernumerary cusps. A dental anomaly, namely dental fusion between a permanent upper left first and second incisors was observed (Fig. 39). These were recovered among the loose, commingled teeth from Tomb SS. Dental fusion is defined as the partial or complete union of two adjacent teeth. The aetiology of dental fusion is unknown, however, it is believed that it could be related to pressure or physical force from the follicles of adjacent teeth, or, e.g., hereditary determinants.<sup>61</sup> At least one other case of dental fusion is known from Cyprus.<sup>62</sup>

### Tomb SS mortuary programmes

The tomb contained articulated, partially articulated, and disarticulated human skeletal remains. These remains reflect complex mortuary programmes, in evidence at other contemporaneous sites in Cyprus. Disarticulated and commingled skeletal elements were recovered from the perimeter of Tomb SS, underneath articulated skeletons. Four episodes of tomb use, at minimum, may be posited based on the human remains from Tomb SS, and their stratigraphic relationships. The partially articulated and disarticulated skeletal remains at the perimeter of the tomb may represent the first inhumations in the tomb. These may have been of a primary or secondary nature (i.e., bodies may have been interred as primary inhumations, with subsequent disarticulation following decomposition and redisposal to make space for further interments, or post-interment activities; or these partially articulated and disarticulated skeletal remains were introduced into the tomb as a secondary deposition, after decomposition elsewhere). The second episode of tomb use may have included the rearrangement of the disarticulated skeletal remains around the perimeter of the tomb followed by the interment of primary inhumations on the top. After the deposition of these primary inhumations (second episode), a third use episode may have taken place, represented by an additional individual skeleton (L139, SK1). This skeleton overlay the primary inhumations of the second use episode. The fourth use episode involved the relocation of this skeleton (L139, SK1) towards the eastern wall of Tomb SS after partial decomposition, with some ligamentous attachments still present, resulting in the deposition of a discrete individual in partial articulation.<sup>63</sup> Subsequently, the tomb was filled with additional tomb gifts.

Long-term reuse of tombs, complex treatments of the dead, and collective secondary treatments frequently occur in the mortuary record of Late Bronze Age Cyprus,<sup>64</sup> including at Hala Sultan Tekke (e.g., Tombs RR and SS). The mortuary pattern observed within Tomb SS corresponds with other contemporaneous sites from the period, including Kourion-Bamboula, Enkomi *Agios Iakovos*, *Agios Iakovos Melia*, and Katydhata, and with the broader mortuary treatment patterns observed during the Late Bronze Age in Cyprus.<sup>65</sup>

### HUMAN REMAINS FROM CHAMBER TOMB TT

Chamber Tomb TT was fully excavated in 2022. Several concentrations of human skeletal remains were identified. These concentrations contained skeletal remains in varying degrees

<sup>59</sup> Fischer & Bürge 2022, 55–58; 2021, 131–134.

<sup>60</sup> Fischer & Bürge 2022, 55–58; 2021, 131–134.

<sup>61</sup> Açkel *et al.* 2018.

<sup>62</sup> Lorentz 2006.

<sup>63</sup> Fischer & Bürge 2021, 131–133.

<sup>64</sup> Keswani 2004, 85–86, 101–102.

<sup>65</sup> Keswani 2004, 93–104; Benson 1972; Gjerstad 1926; Gjerstad *et al.* 1934.

Table 10. “SK” and “Ind” numbers of Chamber Tomb TT with descriptions.

Skeletal remains ID (SK)	Individual ID (Ind)	Description
SK1	IndA	Discrete articulated individual (complete). The individual was found in an extended supine position (N–S)
SK2		Concentration of commingled disarticulated remains
SK3		Concentration of commingled disarticulated remains
SK4	IndB	Discrete articulated individual (partial). The individual was found in a flexed position, on its left side, facing east (NNE–SSW)
SK5		Articulated lower left arm and hand (with silver finger rings N723 and N724); articulated right hand; loose bones and teeth
SK6&7		Concentration of commingled disarticulated remains
SK8	IndC	Partially articulated upper body, found in an extended supine position (SE–NW)
SK9	IndD	Discrete nonadult individual (partial). Burial position could not be determined as the remains were disturbed.
SK10	IndE	Discrete nonadult (complete). The skeleton was found in an extended supine position (ENE–WSW)

of articulation (i.e., articulated, partially articulated, and disarticulated commingled remains). To conduct positional analyses regarding the disposal of human remains within the tomb, contributing towards analyses of mortuary practices, each skeletal concentration/entity was assigned a unique identifier, consisting of a number preceded by “SK” (referring to skeletal remains). Discrete articulated or partially articulated individuals were additionally provided an “Ind” (individual) number (Table 10). Overall, skeletal preservation was moderate to poor and many elements were considerably weathered. Careful documentation of each element or fragment *in situ*, prior to lifting, was prioritized. There appears to have been intentional deposition of commingled remains within different skeletal concentrations. For instance, in the skeletal concentration labelled SK3, specific anatomical elements seem to have been grouped (i.e., ilia deriving from multiple different individuals stacked). The commingled remains from the area designated as SKs 6&7 were delimited by a perimeter made of lower limb bones, primarily femora (Fig. 40). Most of the skeletal remains recovered from Chamber Tomb TT were concentrated in the northern half of the tomb within skeletal concentrations SKs 6&7 and SK3. Based on the stratigraphic sequence the articulated individual SK1\_IndA and the partially articulated individual SK4\_IndB represent the most recent interments. The commingled remains likely represent earlier interments that were intentionally deposited within zones after full or partial decomposition of soft tissues.

### MNI

The minimum number of individuals (MNI) was calculated based on the following criteria: (1) repetition of fragments from the same anatomical position in the skeleton; (2) age incompatibility; (3) considerable differences in size and/or

morphology; and (4) incompatibility of pathologies. In total, the tomb contained a minimum of 25 individuals based on the repetition of the maxillary right permanent second molar as well as the presence of at least three individuals below the expected age for permanent second molar development.

### Age at death

Age at death, defined as the biological age of an individual based on physiological and dental characteristics, was estimated using the following methods: (1) dental development stage;<sup>66</sup> (2) skeletal development stage;<sup>67</sup> (3) morphology of the auricular surface;<sup>68</sup> and (4) morphology of the pubic symphysis.<sup>69</sup> A summary of the age-at-death estimates for the discrete articulated and partially articulated individuals is presented in Table 11. Within the commingled remains from the SK2, SK3, SK5, and SKs 6&7 concentrations, at least eight nonadult individuals of less than eleven years of age are present, based on the presence of eight mandibular right deciduous second molars. The youngest individuals are two perinates.

### Sex

Sex estimation was based on the morphology of the sexually dimorphic features of the skull and pelvis.<sup>70</sup> A summary of the sex estimates for the discrete articulated and partially articulated individuals is presented in Table 11. For the commingled remains from the SK2, SK3, SK5, and SKs 6&7 con-

<sup>66</sup> AlQahtani 2008.

<sup>67</sup> Schaefer *et al.* 2009.

<sup>68</sup> Lovejoy *et al.* 1985.

<sup>69</sup> Brooks & Suchey 1990.

<sup>70</sup> Buikstra & Ubelaker 1994.

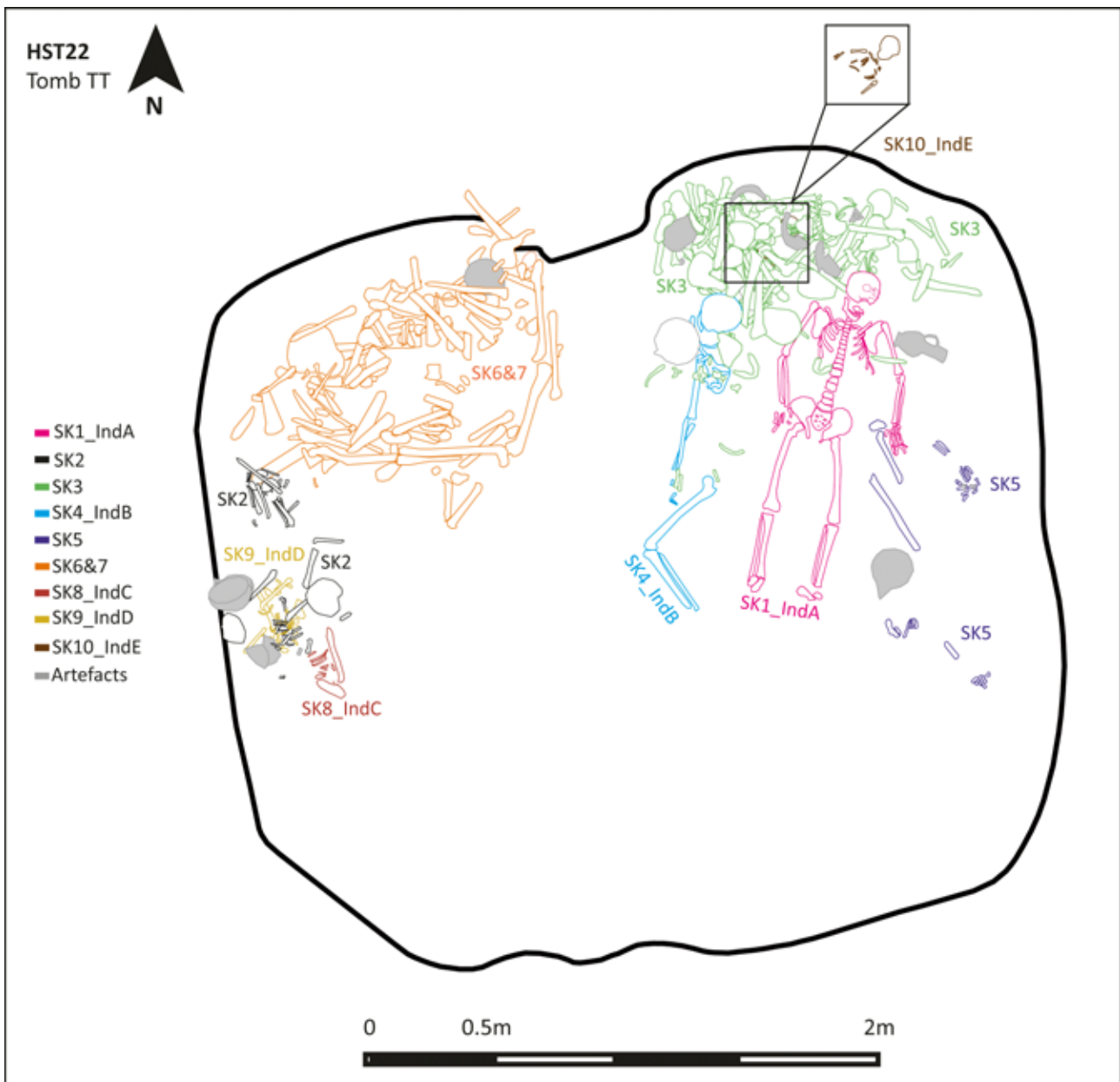


Fig. 40. Human remains from Chamber Tomb TT (drawing by N.M. Branca).

centrations, sex was estimated based on the most numerous element with preserved sexually dimorphic features, the left ilium. The morphology of the sciatic notch assessed in each left ilium suggests that at minimum one female, two probable females, two males, and one indeterminate individual are present. None of the adult skeletal elements from the skeletal concentrations designated as SK2 and SK5 were sufficiently preserved for sex estimation.

### Stature

The estimation of stature was based Mildred Trotter's regression equations for white males and females,<sup>71</sup> using the maximum length measurements of intact long bones. It should be noted that the stature estimates are based on field measurements, as the preservation of the human remains was insufficient (high fragmentation levels) for laboratory measure-

<sup>71</sup> Trotter 1970.

Table 11. Biological profile of discrete articulated and partially articulated individuals from Chamber Tomb TT. cba = cannot be assessed; n/a = not applicable.

Skeletal remains ID (SK)	Individual ID (Ind)	Sex	Age at death	Stature		
				Element	Side	Formula
SK1	IndA	Probable male	40–44 years	Femur	Left	$2.38 (42) + 61.41 \pm 3.27 = 161.37 \pm 3.27$ cm
SK4	IndB	Indeterminate	Adult	Femur	Right	$2.38 (43) + 61.41 \pm 3.27 = 163.75 \pm 3.27$ cm (male formula)
						$2.47 (43) + 54.74 \pm 3.72 = 160.95 \pm 3.72$ cm (female formula)
SK8	IndC	cba	Adult	cba		
SK9	IndD	n/a	Late childhood (6–9 years)	n/a		
SK10	IndE	n/a	7.5 months ( $\pm 3$ months)	n/a		

Table 12. Stature estimates for commingled individuals from Chamber Tomb TT, based on left femora.

Skeletal remains ID (SK)	Maximum length of left femur (cm)	Formula males	Formula females
		[ $2.38$ (max length cm) + $61.41 \pm 3.27$ ]	[ $2.47$ (max length cm) + $54.74 \pm 3.72$ ]
SK3	44	$166.13 \pm 3.27$ cm	$163.42 \pm 3.72$ cm
SK3	42	$161.37 \pm 3.27$ cm	$158.48 \pm 3.72$ cm
SK3	43.5	$164.94 \pm 3.27$ cm	$162.19 \pm 3.72$ cm
SK6&7	43	$163.75 \pm 3.27$ cm	$160.95 \pm 3.72$ cm

ments to be obtained. A summary of the stature estimates for the discrete articulated and partially articulated individuals is presented in Table 11. Stature estimates for the commingled remains (SK2, SK3, SK5, and SKs 6&7 concentrations) were obtained based on field measurements of left femora (Table 12), as they were the most frequently preserved element.

### Dental remains

The dental remains from Chamber Tomb TT include a total of 419 diagnostic permanent teeth of which 217 were maxillary and 202 mandibular. The total number of diagnostic deciduous teeth is 47 including 28 maxillary and 19 mandibular deciduous teeth. Dental pathologies include lesions of dental caries ranging from small to “gross”, as well as linear enamel hypoplasia. In total, 15 permanent teeth display lesions of dental caries (approximately 3.6% of the total permanent teeth). Linear enamel hypoplasia was present on 24 permanent teeth (approximately 5.7% of the total permanent teeth). Furthermore, mild to moderate calculus or tartar was observed on 18 permanent teeth (4.3% of the total diagnostic permanent teeth). Specific observations regarding the dentitions of the discrete individuals SK1\_IndA and SK4\_IndB are included below.

The fully articulated individual SK1\_IndA was recovered with an almost complete dentition. The presence of linear enamel hypoplasia suggests a period of health-related stress in childhood. Caries was present at the distal cemento-enamel junction (CEJ) of the maxillary right second molar and max-

illary left third molar. The maxillary left second molar and maxillary right third molar were lost *ante mortem* as evidenced by the completely remodelled alveolar sockets. Occlusal wear is more pronounced on the right maxillary and mandibular dentition. Combined with the presence of several teeth with chipped enamel (mandibular right canine and second premolar as well as maxillary left canine) it is possible that the individual was relying more heavily on the right side of the mouth for masticatory or other activities.

The partially articulated individual SK4\_IndB only contained partial maxillary dentition, primarily from the right side. Lesions of dental caries were present at the CEJ of the maxillary left first incisor and maxillary right second molar.

Dental nonmetric traits observed in Chamber Tomb TT teeth include Carabelli's trait, shovelling, supernumerary roots, supernumerary cusps, interruption grooves, and expression of the tuberculum dentale (Table 13). Carabelli's trait is identified by the presence of an additional cusp on the mesiolingual aspect of the crown of maxillary molars.<sup>72</sup> Shovelling is typical of the maxillary incisors and is identified by the presence of distinct ridges on the lingual edges of the tooth crowns, giving the tooth a distinct shovel-like shape.<sup>73</sup> Similarly, interruption grooves are a nonmetric feature typical of maxillary incisors, more commonly the second incisors. These

<sup>72</sup> Edgar 2017; Hillson 2005.

<sup>73</sup> Edgar 2017; Hillson 2005.

Nonmetric trait	Permanent/ deciduous	Maxillary/ mandibular	Tooth type	Side	Number of teeth with the trait
Carabelli's trait	Permanent	Maxillary	M1	Right	3
				Left	3
	Deciduous	Maxillary	M2	Right	1
				Left	1
Shovelling	Permanent	Maxillary	I2	Left	3
Supernumerary roots	Permanent	Maxillary	M3	Left	1
Supernumerary cusps— metaconule	Permanent	Maxillary	M2	Right	1
				Left	1
Interruption groove	Permanent	Maxillary	I2	Right	1
			I2	Left	1
Tuberculum dentale	Permanent	Maxillary	I1	Left	2
				Right	1
“Peg” teeth	Permanent	Maxillary	I/C	cba	1
	Permanent	cba	M	cba	1

Table 13. Dental nonmetric traits occurring in Chamber Tomb TT. *cba* = cannot be assessed.

grooves meet or cross the cingulum and may extend to the root.<sup>74</sup> Some teeth have supernumerary roots. Supernumerary cusps such as the metaconule—an additional cusp on the distal aspect of the crown of maxillary molars between the metacone and the hypocone—commonly occur in molar teeth. The tuberculum dentale is one or several ridges that appear on the lingual aspect of primarily incisors and canines on or near the cingulum.<sup>75</sup> Two microdont, peg-shaped teeth were found in the area of SK3 (Fig. 41). Microdontia is a genetic anomaly of the crown shape and size, whereby the tooth crown is smaller than usual, or small in relation to other teeth.<sup>76</sup> The condition typically affects one or two teeth, commonly the lateral (second) maxillary incisors and third molars. However, in some cases all teeth can be affected, a condition known as generalized microdontia. One such case was discovered in the Cypriot Middle Chalcolithic (3500–2800 BC) site of Souskiou-Laona.<sup>77</sup>

### Skeletal pathologies

The skeletal pathologies of the discrete individual SK1\_IndA as well as those observed on the commingled bones from skeletal concentrations SK3 and SKs 6&7 are described below. No macroscopically observable skeletal pathologies were present among the remains from SK2, SK4\_IndB, SK5, SK8\_IndC, SK9\_IndD, and SK10\_IndE.

**SK1\_IndA:** Small meningiomas are evidenced by the presence of smoothed-out cavities on the endocranial surface of the left parietal bone, fed by an enlarged meningeal ves-

sel.<sup>78</sup> Spinal pathologies include mild vertebral osteoarthritic changes, as well as bony outgrowths at the edges of vertebral bodies (may be indicative of intervertebral disc disease), primarily focused on the lumbar spine. Several Schmorl's nodes were noted in the lower spine, with particularly large cavities on the T11 and T12 vertebrae.

**SK3:** The frontal bone of a nonadult individual recovered from this concentration of commingled skeletal remains displays porosity on the orbital roof (*cribra orbitalia*). Among the commingled vertebrae, pathological lesions include Schmorl's nodes, bony outgrowths at the edges of vertebral bodies, ossification of the ligamentum flavum, and osteoarthritic changes. Two distal foot phalanges from opposite sides (left and right) display bone spurs on the disto-medial aspect of the superior surface. Although these were recovered from a commingled context, similarity of the pathological lesions suggests that they derive from a single individual. One right navicular bone displays abnormal extra-articular bone growth on the supero-medial aspect, possibly consistent with osteoarthritic changes, though not enough of the bone is preserved for definitive analysis. Similar bony growth was present on the disto-medial or disto-lateral aspect of a proximal foot phalanx which cannot be sided.

**SKs 6&7:** Among the commingled remains recovered from the skeletal concentration designated as SKs 6&7, commonly observed vertebral pathologies include Schmorl's nodes and osteoarthritic changes. Some vertebral spinous processes also display evidence of ossification of the ligamentum flavum. Further, the proximal epiphysis of a right femur displays moderately advanced osteoarthritic changes, including considerable alteration of the joint contour (Fig. 42).

<sup>74</sup> Edgar 2017.

<sup>75</sup> Edgar 2017.

<sup>76</sup> Soxman *et al.* 2019.

<sup>77</sup> Lorentz *et al.* 2021b.

<sup>78</sup> Waldron 2009.



Fig. 41. Peg-shaped molar with elongated crown and three small cusps (left); peg-shaped tooth, possibly a maxillary canine or incisor (right). From Chamber Tomb TT (Image by N.M. Branca).

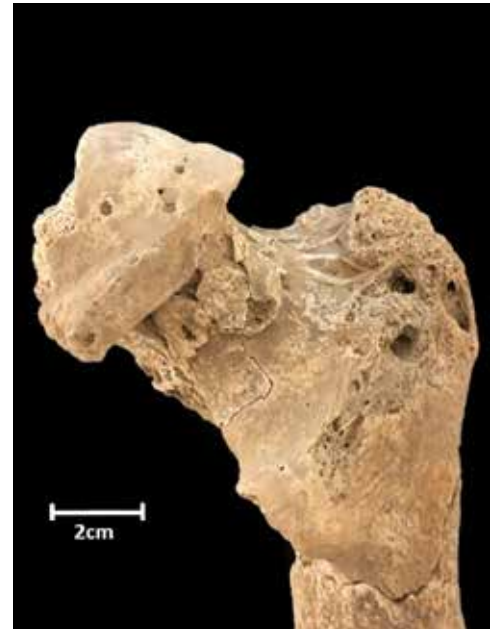


Fig. 42. Proximal end of a right femur from Chamber Tomb TT with osteoarthritic changes (Image by N.M. Branca).

### Summary of Chamber Tomb TT human remains

The tomb contained a minimum of 25 individuals based on the repetition of the maxillary right permanent second molar as well as the presence of at least three individuals below the expected age for permanent second molar development. The tomb contained individuals of all ages, ranging from perinate to old adult. In total, a minimum of one female, two probable females, two males, one probable male, and two indeterminate individuals are represented. Stature estimates range from  $158.48 \pm 3.72$  cm to  $166.13 \pm 3.27$  cm.

### HUMAN REMAINS FROM CHAMBER TOMB UU

The following sub-sections detail the results of the bioarchaeological analyses of the human skeletal remains recovered during the 2022 excavation season of Chamber Tomb UU, which is only partly excavated.

The first human skeletal remains within the area of Chamber Tomb UU were found on the surface of an area identified as a magnetic anomaly during a large-scale magnetometer survey of the site.<sup>79</sup> These human bones showed signs of having been exposed to surface weathering events and farming activities (i.e., ploughing), and were consequently fragmentary, in extremely poor preservation state, and mostly undiagnostic.

A 10 (east to west) × 4 m (north to south) area was delineated based on surface finds and magnetometer mapping, and excavation began in a 4 × 4 m trench in the northern half of the area. Human skeletal remains were immediately located in the north-eastern corner of the trench which had been disturbed by ploughing activities. In the modern topography of the site the tomb is currently positioned on an upper portion of a gradual slope, though in antiquity the human remains of Chamber Tomb UU likely lay under a thicker layer of soil. Weathering, erosion and continued farming activities, most notably ploughing with heavy machinery, have presumably exposed the upper levels of the deposits containing human remains to significant taphonomic processes (both natural and anthropogenic). The top-most deposits have presumably been displaced, with heavy degradation of the human skeletal remains found on the surface and within the immediately underlying upper deposits (Fig. 43).

Two concentrations of disarticulated human skeletal remains were found in Chamber Tomb UU, the first against the northern perimeter/wall of the tomb (L300, L301, L304), and the second (L305) positioned south of the first concentration (Fig. 43). The upper levels of the deposit lining the northern perimeter of the tomb were heavily affected by ploughing activities, with the bones in the upper strata (L300) seemingly dragged out of context by the plough, reflected also by their fragmentary and fragile condition. The human skeletal remains in the lower deposit (L301) of the northern con-

<sup>79</sup> Fischer & Bürge 2022, 7.

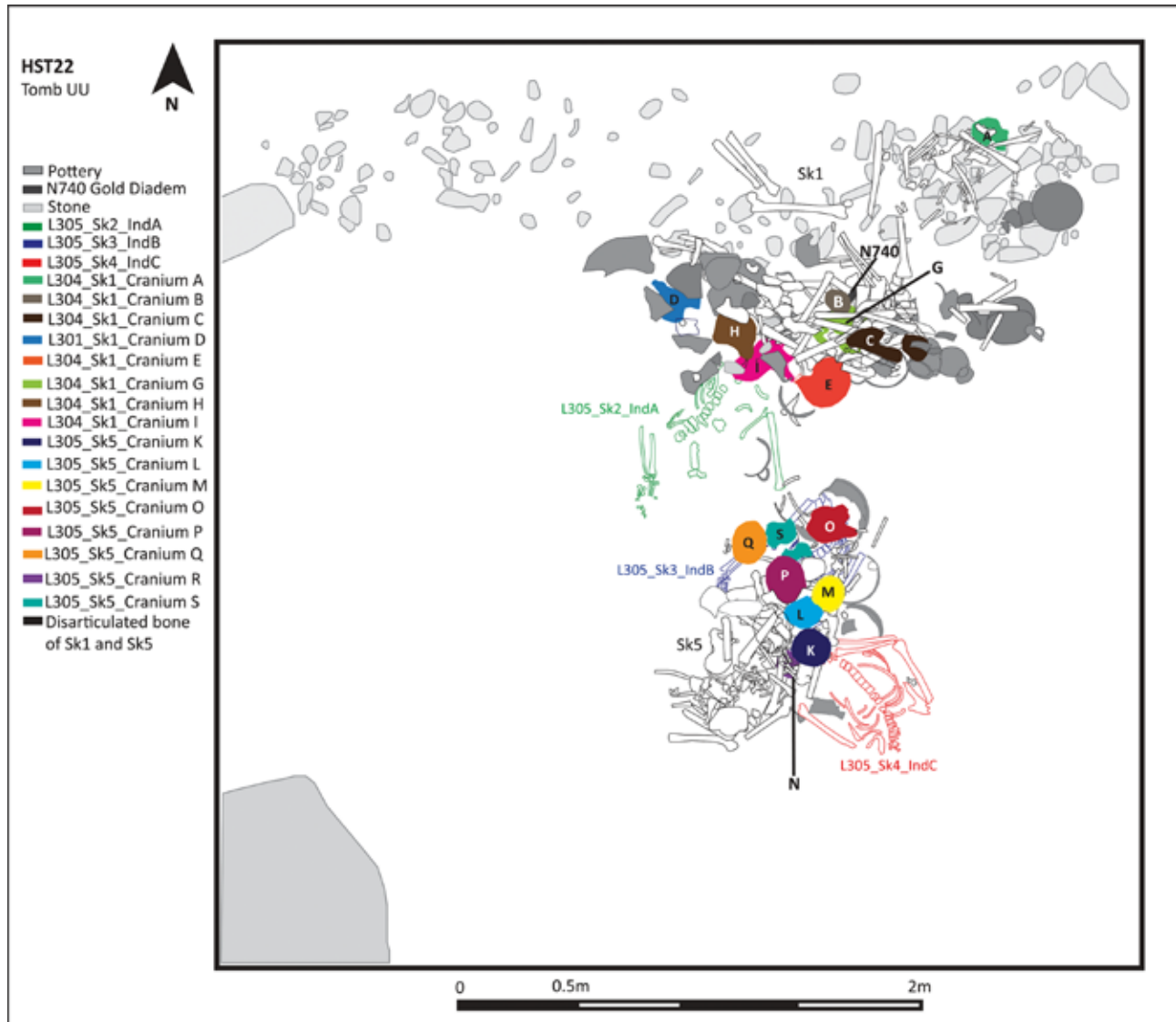


Fig. 43. Human skeletal remains recovered from Chamber Tomb UU (drawing by B. Casa).

centration were not affected by ploughing and were recovered in a better state of preservation.

The lower deposits of the northern concentration comprised disarticulated skeletal remains that had been deliberately stacked along the northern perimeter of the tomb (L301, L304). More specifically, ilia of individuals of different ages at death (i.e., ilia belonging to both adults and nonadults) were stacked on top of each other within the concentration of disarticulated bones. A similar pattern was observed with the grouping of crania in the lower deposits. The other concentration of bones (L305) contained disarticulated skeletal remains in the upper deposits, which also display some evidence of intentional manipulation. A total of eight crania

were found in this locus, mostly grouped together, and similarly to L304, skeletal elements such as humeri and ilia were stacked or positioned together. Underneath the disarticulated bones of L305, three partially articulated skeletons, all three including an articulated torso and arm bones, were identified, positioned on a surface (L305: SK2 IndA, SK3 IndB, SK4 IndC; *Table 14*).

In addition to the three partially articulated skeletons (*Table 14*) a minimum of 16 crania (*Table 15*) were found in Chamber Tomb UU. No crania were recovered in association with the three partially articulated skeletons (L305: SK2 IndA, SK3 IndB, SK4 IndC).

Table 14. Biological profile of partially articulated skeletons from Chamber Tomb UU. cba = cannot be assessed; n/a = not applicable.

Locus (L); Skeletal remains ID (SK); Ind ID	Degree of articulation	Age at death		Sex	Stature				
		Adult / Nonadult	Years		Bone	Max length of bone	Method	Formula	Stature estimate
L305 SK2 IndA	Partially articulated	Adult	cba	Male?	Right first metacarpal	4.55 cm	Meadows & Jantz 1992	$46.62 \times 1.659$ $+ 91.77$ $\pm 5.52$	169.11 $\pm 5.52$ cm
L305 SK3 IndB	Partially articulated	Adult	cba	cba	Right radius	21.9 cm	Sjøvold 1990	$4.03 \times 21.9 +$ $69.96 \pm 4.98$	158.2 $\pm 4.98$ cm
L305 SK4 IndC	Partially articulated	Nonadult	14–16 years ( $<14$ years female, $<16$ years male)	n/a	n/a	n/a	n/a	n/a	n/a

Locus	Cranium ID	Age at death		Sex
		Adult/Nonadult	Years	
L301	Cranium D	Adult	18–22	Male
L304	Cranium A	Adult	24–30	Probable female
L304	Cranium B	Adult	18–22	Probable female
L304	Cranium E	Adult	24–30	Female
L304	Cranium G	Adult	35–40	Probable male
L304	Cranium I	Adult	cba	Probable female
L304	Cranium H	Adult	20–24	Probable female
L304	Cranium C	Adult	16–20	Probable male
L305	Cranium I	Adult	18–22	Probable female
L305	Cranium K	Nonadult	$<7.5$	n/a
L305	Cranium L	Adult	18–22	Male
L305	Cranium M	Nonadult	9.5	n/a
L305	Cranium O	Adult	18–22	Probable female
L305	Cranium Q	Adult	18–22	Female
L305	Cranium R	Nonadult	$<1.5$	n/a
L305	Cranium S	Adult	20–24	Indeterminate

Table 15. Biological profile of discrete crania recovered from Chamber Tomb UU. cba = cannot be assessed; n/a=not applicable.

## MNI

The minimum number of individuals (MNI) was calculated on the basis of the following criteria: (1) repetition of fragments from the same anatomical position in the skeleton; (2) age incompatibility; (3) considerable differences in size and/or morphology; and (4) incompatibility of pathologies.<sup>80</sup> The MNI for Chamber Tomb UU was calculated based on dentition, and in particular, the mandibular right and left first molars. The MNI for Chamber Tomb UU is 19, including four nonadults and 15 adults.

## Age at death

The estimation of age at death for Chamber Tomb UU human remains was conducted using dental development, dental wear, and epiphyseal fusion. Dental development, in the context of age estimation, was assessed using the method developed by Isaac Schour and Maury Massler.<sup>81</sup> In the absence of more reliable age-at-death indicators in the skeleton, maxillary dental wear was scored in adult crania using C. Owen Lovejoy's method.<sup>82</sup> It is noted that there is currently no population-specific dental wear data for Cyprus. Where observable, epiphyseal fusion was used for the estimation of age at

<sup>80</sup> Bello & Andrews 2006; Robb 2016; Lorentz *et al.* 2021a.

<sup>81</sup> Schour & Massler 1941.

<sup>82</sup> Lovejoy 1985.

Nonmetric trait		Mandibular/ Maxillary	Tooth type	Side	Number of teeth displaying the trait
Carabelli's trait		Maxillary	M1	right	2
				left	2
			M2	right	1
				left	1
			dm2	right	1
			Shovelling		Maxillary
Supernumerary roots		Mandibular	C	left	1
			PM1	right	1
Supernumerary cusps	Metaconule	Maxillary	M2	right	1
				left	1
	Hypoconulid	Mandibular	M2	right	1
				left	1
	Parastyle	Maxillary	M3	left	1

Table 16. Nonmetric traits present in dental remains from Chamber Tomb UU.

death in nonadults using the guidelines of Maureen Schaefer, Sue Black, and Louise Scheuer.<sup>83</sup> Epiphyseal fusion of L305 SK4 indicates an estimated age at death of 14–16 years (*Table 15*). Dental development data indicates 15 adults and four nonadults. The average age at death of adults based on dental wear is within early adulthood at 22 years, and the age range for nonadults using dental development spans from 1.5 to 9.5 years (*Table 15*).

### Sex

Where possible, sex was estimated by assessing sexually dimorphic skeletal elements.<sup>84</sup> Crania were used for sex estimation as they were the most numerous element with preserved sexually dimorphic features within Chamber Tomb UU. Of the minimum of 16 crania, a total of 13 were complete enough for sex estimation. The sex estimates for these crania are: two females, six probable females, two males, two probable males, one individual of indeterminate sex (*Table 15*). Further, in the absence of cranial or pelvic bones, the presence of bilateral rhomboid fossae on the clavicles of L305 SK2—a nonmetric trait that most frequently presents in males—may be consistent with a hypothesis of a male or probable male sex (*Table 15*).<sup>85</sup>

### Stature

Stature was estimated for partially articulated individuals based on available stature diagnostic bones (larger long bones and metacarpals), and the most numerous diagnostic disarticulated skeletal element within the commingled disarticulated

bones. Stature estimation was based on larger long bones.<sup>86</sup> For metacarpals, Lee Meadows' and Richard L. Jantz' definition was used.<sup>87</sup> Given that some individuals were partially articulated, represented only by the torso and arm bones, it is possible that some of the disarticulated commingled long bones may have belonged to these individuals. Consequently, only one or the other of the following (but not both) can be used for any further statistical or other analyses: (1) the stature estimates based on the most numerous commingled bone suitable for stature estimation (femur); or (2) stature estimates derived from the upper limb bones of the partially articulated skeletons. L305 SK2, a possible male, has an estimated stature of  $169.11 \pm 5.52$  cm, and L305 SK3, whose sex could not be estimated, had an average estimated stature of  $158.2 \pm 4.98$  cm (*Table 14*). When considering the disarticulated bones, two right femora were preserved for measurement and revealed stature estimates of  $166.18 \pm 4.49$  cm and  $154.26 \pm 4.49$  cm.

### Dental remains

Chamber Tomb UU diagnostic dental remains recovered include 347 permanent teeth, of which 178 are maxillary and 169 mandibular. The diagnostic deciduous teeth recovered from Chamber Tomb UU include 32 deciduous teeth, of which 20 are maxillary and 12 mandibular. A total of 14 teeth (all permanent) display carious lesions, representing *c.* 4% of the diagnostic permanent teeth. These lesions ranged from small to gross (*i.e.*, large). Fifty-four permanent teeth (15.6%) display calculus/tartar ranging from mild to considerable. Linear enamel hypoplasia—a defect of the dental enamel associated with health-related stress at the time of dental devel-

<sup>83</sup> Schaefer *et al.* 2009.

<sup>84</sup> Buikstra & Ubelaker 1994.

<sup>85</sup> Rogers *et al.* 2000.

<sup>86</sup> Sjøvold 1990.

<sup>87</sup> Meadows & Jantz 1992.

opment—was also identified on 30 permanent teeth (8.6% of the diagnostic permanent dentition). Dental nonmetric traits include Carabelli's trait, shovelling, supernumerary roots, and supernumerary cusps (*Table 16*).

The most commonly observed dental nonmetric trait among the teeth from Chamber Tomb UU is Carabelli's trait. The trait is identified by the incidence of an additional cusp on the mesio-lingual aspect of the crown of maxillary molars.<sup>88</sup> It was identified on two right and two left maxillary first molars, one right and one left maxillary second molar, and one maxillary deciduous second molar. Shovelling is a trait common in maxillary incisors and refers to pronounced ridges on the mesial and distal edges of the tooth crown.<sup>89</sup> In the case of Chamber Tomb UU the trait was present on two right maxillary incisors. Supernumerary roots were noted on two teeth, a mandibular right canine and a mandibular right third premolar. In addition, several teeth displayed supernumerary cusps. One maxillary right and one left second molar possessed an additional fifth cusp known as a metacone—it occurs on the distal aspect of the tooth crown between the metacone and the hypocone.<sup>90</sup> Further, two mandibular second molars of opposite sides also presented with a fifth cusp known as the hypoconulid. Lastly, an additional cusp on the buccal surface of the mesiobuccal cusp, known as the parastyle, was present on one maxillary left third molar.<sup>91</sup>

#### Skeletal pathologies and nonmetric variants

Pathological lesions and changes identified in the skeletal remains from Chamber Tomb UU include osteoarthritic changes, Schmorl's nodes, and the ossification of the ligamentum flavum. Bilateral rhomboid fossae were identified on the clavicles of L305 SK2. Rhomboid fossae are a skeletal nonmetric variant that occurs on the clavicle for the attachment of the costoclavicular ligament, and most frequently it occurs in males, particularly in younger males, with the largest fossae in males between 20 to 30 years of age.<sup>92</sup>

#### Summary of Chamber Tomb UU human remains

The human skeletal remains from Chamber Tomb UU included three partially articulated individuals, as well as disarticulated commingled skeletal elements. An MNI of 19 individuals was recorded, comprising four nonadults and 15 adults. Sex estimates indicate that both females and males were interred within the tomb. Age at death estimates show

that a wide age range of individuals is represented in the tomb, including infants, children, adolescents, and adults. The stature estimates of individuals interred in Chamber Tomb UU range from 154 cm to 169 cm. Though no conclusive evidence is available, the discovery of three partially articulated skeletons in Chamber Tomb UU, with no associated cranial remains, and at least 16 crania (MNI 16) without clearly associated postcranial remains is not inconsistent with the idea of cranial removal posited for other contemporary Late Bronze Age sites in Cyprus, such as Pendaria *Mandres*, Katydhata, and Politiko *Ayios Iraklidhios*.<sup>93</sup> Further excavation of Chamber Tomb UU is expected to result in the discovery of further human remains. These and the already recovered human remains reported on here will need to be considered together to arrive at a conclusive analysis of the Chamber Tomb UU mortuary assemblage.

#### BIOARCHAEOLOGICAL CONCLUSIONS, SEASON 2022

This report summarizes the results of macroscopic, metric, and contextual analyses of the human remains from Pit Tomb L198, and Tombs TT and UU, with additional summary of Tomb SS. Comprehensive and definitive analyses of these remains in their site and tomb contexts will require the previously excavated and future human remains to be recovered from the site to be considered together. Some clear patterns of interest are already apparent however, regarding mortuary analysis: (1) individuals of all ages, from perinate to old adults are interred in the tombs; (2) both females and males are interred within tombs; (3) fleshed bodies are introduced to the tombs in successive episodes of interments; (4) following (partial) decomposition of soft tissues, skeletal elements or partially articulated body parts are moved, presumably in preparation for the tombs to receive further interments; and (5) disposal of disarticulated and partially articulated body sections is intentional and organized, rather than haphazard, involving arrangement of skeletal elements in zones (such as in Chamber Tomb TT), stacking of specific skeletal elements (e.g., ilia in Tombs TT and UU), or grouping of skeletal elements, such as crania. Further analyses are ongoing, including those enabled by synchrotron radiation approaches, exploring evidence, for instance, for human metal exposure (SR-micro-XRF), as well as pathologies (SXCT) and organic compound preservation (SR-FTIR), requiring high-resolution data in micrometre and/or nanometre scales.

<sup>88</sup> Edgar 2017; Hillson 2005.

<sup>89</sup> Edgar 2017; Hillson 2005.

<sup>90</sup> Edgar 2017; Hillson 2005.

<sup>91</sup> Edgar 2017; Hillson 2005.

<sup>92</sup> Rogers *et al.* 2000.

<sup>93</sup> Karageorghis 1965; Gjerstad 1926.

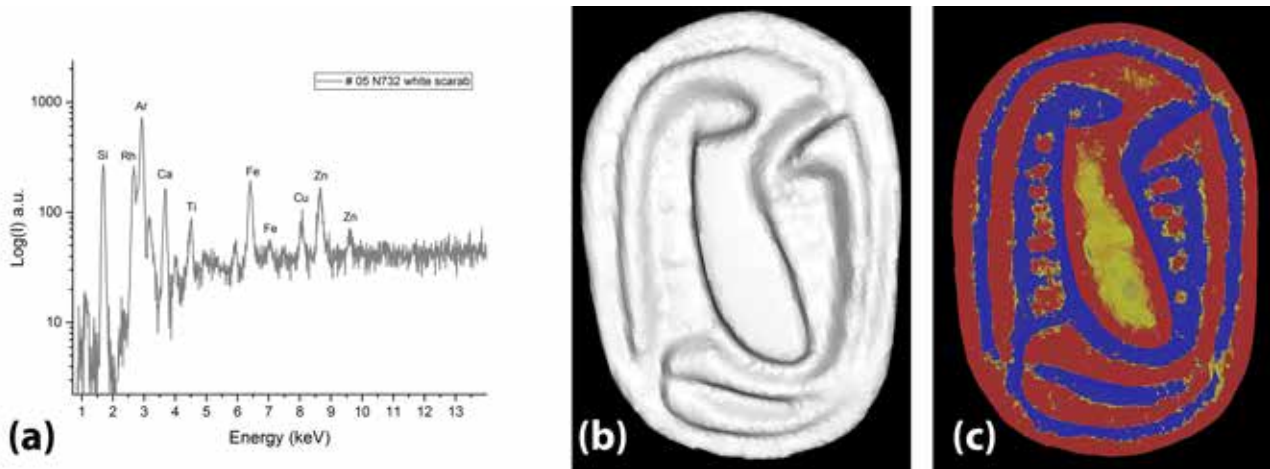


Fig. 44. Analysis of scarab N732: (a) XRF spectrum of the base material (copyrights: Svetlana Gasanova), (b) visualization of the N732 three-dimensional model with light direction change to enhance the engravings' shape, and (c) visualization of the N732 three-dimensional model with MeshLab "Radiance scaling" shader with curvature colour enhancement (copyrights: Valentina Vassallo and Rahaf Orabi).

## Appendix 2. Technical examination of three scarabs from Hala Sultan Tekke by 3D shape and material analyses

BY SVETLANA GASANOVA, VALENTINA VASSALLO, RAHAF ORABI, PANAGIOTIS IOANNOU & SORIN HERMON<sup>94</sup>

### INTRODUCTION

This report presents the preliminary results of the technical analyses of three scarabs—N732, N794, and N782—from the 2022 excavation season at Hala Sultan Tekke. This examination aims to shed light on the modes of production, techniques of manufacture, and the current condition of these artefacts.

The applied methodology combines 3D documentation for 3D shape analysis, as well as advanced analytical techniques including digital microscopy, X-Ray Fluorescence spectroscopy (XRF), Visible-Induced Infrared Luminescence (VIL) imaging, Fourier-Transform Infrared spectroscopy (FTIR), X-Ray Diffraction analysis (XRD) spectroscopy, and Scanning Electron Microscopy (SEM).

<sup>94</sup> Affiliations: Svetlana Gasanova, Valentina Vassallo, Rahaf Orabi, and Sorin Hermon: Andreas Pittas Art Characterization Laboratories (APAC), Science and Technology for Archaeology Research Center (STARC) of The Cyprus Institute, Konstantinou Kavafi 20, 2121 Aglantzia, Nicosia, Cyprus. Panagiotis Ioannou: The Powder Technology Laboratory, 203B and 002A Latsia Campus, University of Cyprus.

	Maximum sizes (cm)			d	Wt (g)
	L	W	H		
N732	1.18	0.83	0.56	1.6	0.9
N794	1.38	1.04	0.56	1.6	0.9
N782	1.53	0.99	0.67	front (1.9 × 2.1), back (1.7 × 3)	

Table 17. Measurements of the scarabs (L: Length, W: Width, H: Height, d: Diameter of the hole, Wt: Weight). It was not possible to weigh scarab N782 due to its high fragility.

### RESULTS AND DISCUSSION

#### N732

Scarab N732 is made of a white material with no traces of painted decoration according to the microscopic investigation. The XRF spectrum of the base material (Fig. 44a) shows the low intensity of all XRF lines suggesting that the scarab's material is comprised of low-Z elements. Steatite (white magnesium silicate) or ivory/bone (organic) can be proposed as possible materials of N732. The carved decoration of N732 was studied through 3D shape analysis. After the 3D documentation with the structured light scanner, an accurate 3D model representing the object was obtained.<sup>95</sup> In this specific case, the 3D scanner could acquire one of the most challenging parts of such an artefact, the small cross-cut hole. The scanner's light could not reach the most inner part, but it acquired the shape of the antithetic holes well. Specifically, the digital measurements of the diameters (1.6 mm) show the same value and the perfect axially of the cavities (Table 17). The digital

<sup>95</sup> Georgopoulos *et al.* 2010.

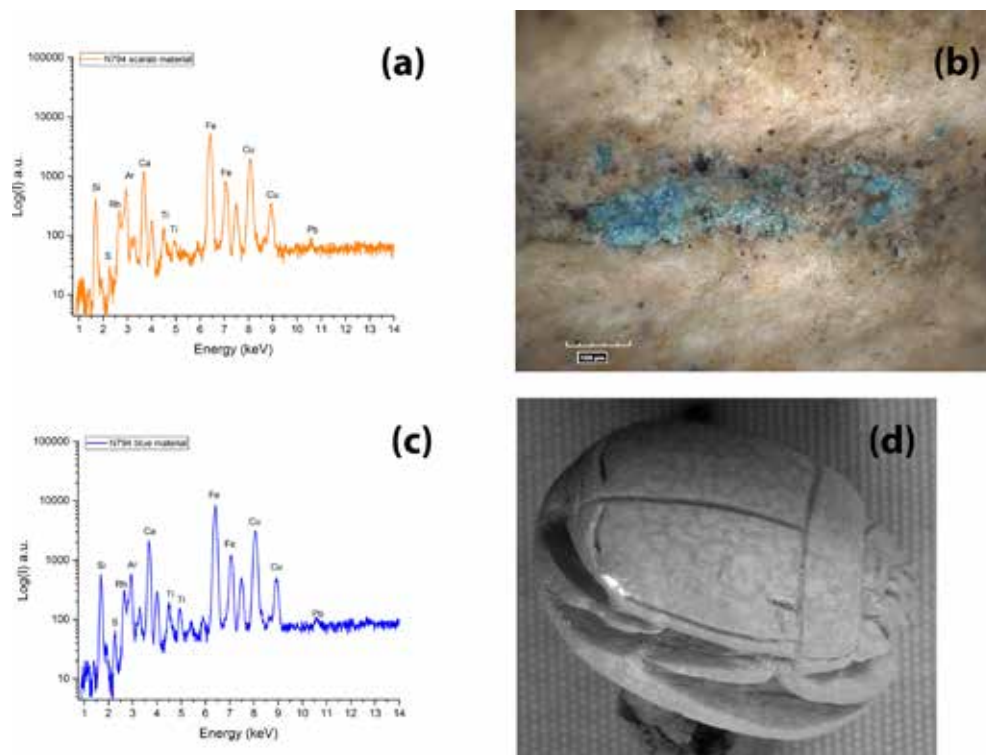


Fig. 45. Non-invasive analysis of scarab N794: (a) XRF spectrum of the base material, (b) micrograph showing coarse angular blue crystals; (c) XRF spectrum taken from the blue area showing the presence of Cu and Si lines, and (d) VIL image showing bright fluorescence of the blue material under near-infrared light characteristic of Egyptian blue (copyrights: Svetlana Gasanova and Ropertos Georgiou).

positioning of the scarab on its central axis in visualization software, for instance MeshLab,<sup>96</sup> allows one to assume that the artisan obtained the cavity by drilling the object from one direction only because of the perfectly straight hole.

3D shape analysis was also beneficial for better visualization of the engravings. The application of 3D filters clearly shows the shape of a uraeus, the stylized upright representation of the rearing cobra, and the Ma'at-feather. The filters emphasize the incised lines representing the cobra stripes, stressing the artist's elevated level in rendering a realistic representation of the animal (Fig. 44b, c). The attention to detail is visible also on the other incised features of the carapace.

## N794

Microscopy observations and XRF analysis (Fig. 45a) of the base material of scarab N794 revealed a pattern similar to N732, e.g., the presence of only low-Z elements suggesting that it could also be made of such materials as steatite or ivory/bone. Close microscopy observations of the surface of N794 revealed the presence of a blue material inside one of its carved lines (Fig. 45b). The blue material has coarse angular crystals, and the XRF spectrum taken from that spot shows intense copper lines (Fig. 45c). The VIL imaging analysis allowed us

to unambiguously identify the nature of the copper-blue pigment, which appeared to be Egyptian blue ( $\text{CaCuSi}_4\text{O}_{10}$ ). This conclusion was possible based on the characteristic photoluminescence of Egyptian blue induced by near-infrared light, which enabled the identification of tiny amounts of this material on archaeological objects (Fig. 45d). This raised the question whether the Egyptian blue belongs to the scarab or represents accidental deposition. Among the objects from the same context is a blue bead (see N793, Fig. 13 in the main report), the colour of which matched the colour of the blue pigment on the scarab. According to the contextual information, this bead was found close to the scarab. VIL imaging of the bead revealed that it is also made of Egyptian blue. Thus, it is possible to conclude that scarab N794 was accidentally contaminated with the blue pigment.

Scarab N794 was also documented with a structured light scanner that produced a 3D model of the small scarab. Because of the deep incisions characterizing the shape of the artefact, the scanner could not completely cover the shape of the small cross-cut holes. Digital measurements of both the holes taken at their external edges showed a diameter of 1.6 mm (Table 17). The visualization in MeshLab of the object positioned on its central axis, also in this case shows a perfect antithetic correspondence of the cavities, suggesting that the artist might have obtained them by drilling in one direction.

Moreover, computer vision techniques (e.g., light filters and shaders) were applied to the 3D model of scarab N794

<sup>96</sup> Cignoni *et al.* 2008.

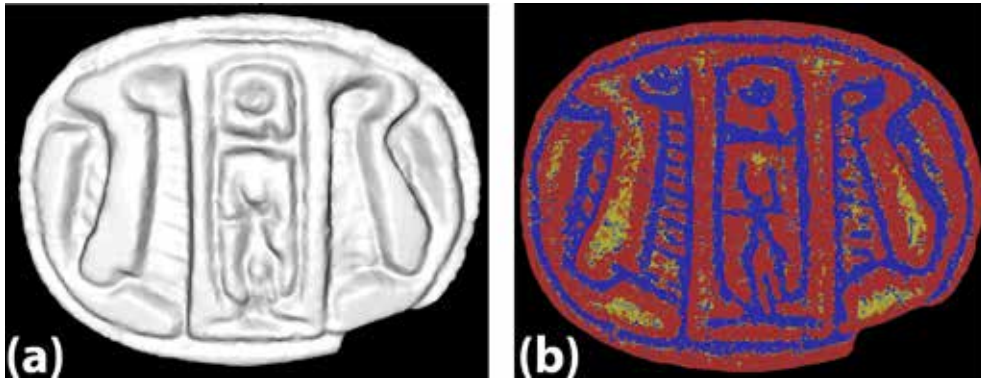


Fig. 46. Visualization of the N794 3D model with: a) light direction change to better isolate the shapes from the background; and b) MeshLab “Radiance scaling” shader with curvature colour enhancement (copyrights: Valentina Vassallo and Rabaf Orabi).

to better identify the engraved shapes visible on the base of the scarab. The light change direction in MeshLab allowed us to better isolate the figures from the background (Fig. 46a). The successive application of the “Radiance scaling” shader with curvature colour enhancement made the motif clearer. The 3D shape enhancement shows among other motifs two lateral uraei (Fig. 46b). The shapes and the artistic representation of the antithetic cobras with incised stripes are similar to the motif on N732.

### N782

Microsamples were collected from scarab N782 after it fractured (see main report) and analysed with a SEM and XRD to obtain information on the crystalline structure of the material (Tables 18, 19). This scarab is made of a translucent glass-like green material. XRF spectra taken from the base material show intense copper and silicon lines (Fig. 47a). Among other elements are lead, titanium, calcium, and iron. Microscopy observations demonstrated that the material is heavily damaged with pores, and cracks (the scarab fractured although properly handled) due to corrosion (Fig. 47b, c). These results suggest that the scarab is made of a copper-containing green material such as glass or faience. More precise identification is not possible with the analytical techniques used. Regarding the white material inside, it is possible to assume that it was formed as a result of a reaction with the environment.

The SEM image taken from the green material shows vitreous material with multiple pits (Fig. 48b), which could be explained by the corrosion due to its exposure to environmental conditions (e.g., pH-related or salty soil). The visible pits on the SEM images seem to be air bubbles in the green material that were created when it was in liquid form. SEM images taken from the outer layer of the scarab, which is paler than the inner layer, show developed porosity. This layer consists of multiple sublayers, which could be explained by multiple stages of corrosion.

The combined results of the digital microscopy, XRF, XRD and SEM of scarab N782 (Fig. 48) suggest that it is made of a glass material, the green colour of which is caused by the presence of copper. Throughout time, the scarab underwent corrosion, which caused degradation of the scarab material and the creation of multiple corroded layers. This, in turn, caused the formation of cracks and gaps between the layers. Previous studies of glass scarabs report comparable results regarding the corrosion of the glass material, which causes the loss of stability and disintegration of scarabs.<sup>97</sup>

The digital documentation of the scarab was highly beneficial. The object was particularly difficult to handle due to its poor state of preservation and it was impossible to take any exact measurements of the artefact (Table 17). The digital documentation produced a 3D model of the artefact, as it was before the natural disintegration of the material (Fig. 49a). The study of the digital model helped to identify the corroded details of the carapace that originally might have been incised after the glass had cooled and then polished. These incisions are slightly visible to the naked eye because of the deterioration of the material. The direction change of the light through the MeshLab visualization software allows enhancement of these lines and highlights the efforts of the maker to detail the artefact. The naked eye observation did not enable the detection of other incisions. The visualization, both with microscope and 3D analysis, further highlighted the lack of any interpretable inscriptions or engravings on its base. The enhancement of the 3D surface with Meshlab shaders (e.g., “Minnaert” and “Radiance scaling”) confirmed the assumption (Fig. 49b). Specifically, the visualization through the colourized curvature of the 3D model allows the detection of a uniform, spread yellow colour indicating the base; the red and blue peaks represent differences in height respect to the base. Their lack of uniformity confirms that there were

<sup>97</sup> Fletcher *et al.* 2008.



Fig. 47. Non-invasive analysis of scarab N782: (a) XRF spectrum of the base material, (b) micrograph showing corroded surface of the scarab, and (c) micrograph taken after the scarab fell apart exposing its multiple layers and a white material inside (copyrights: Svetlana Gasanova).

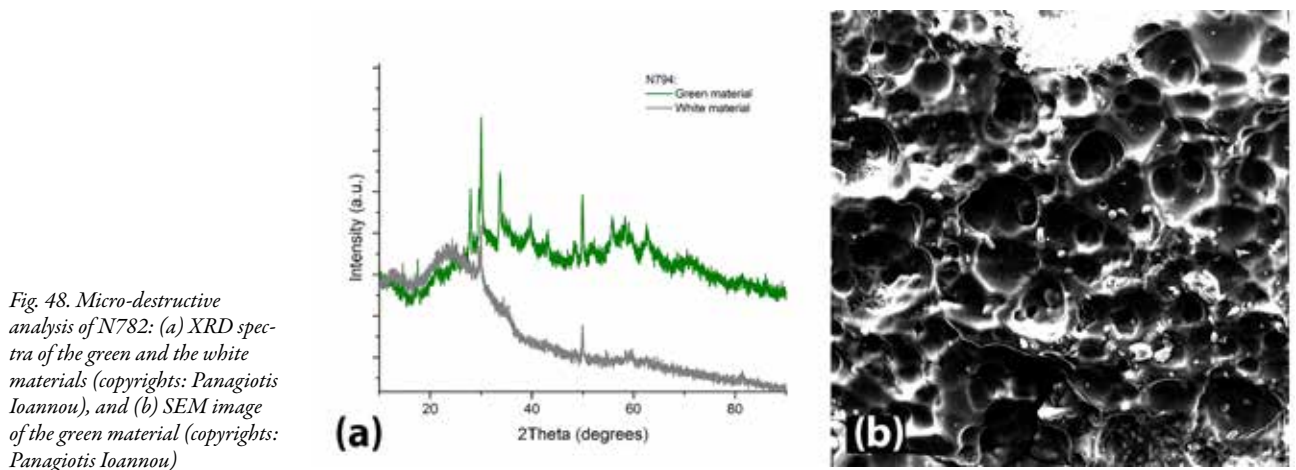


Fig. 48. Micro-destructive analysis of N782: (a) XRD spectra of the green and the white materials (copyrights: Panagiotis Ioannou), and (b) SEM image of the green material (copyrights: Panagiotis Ioannou)

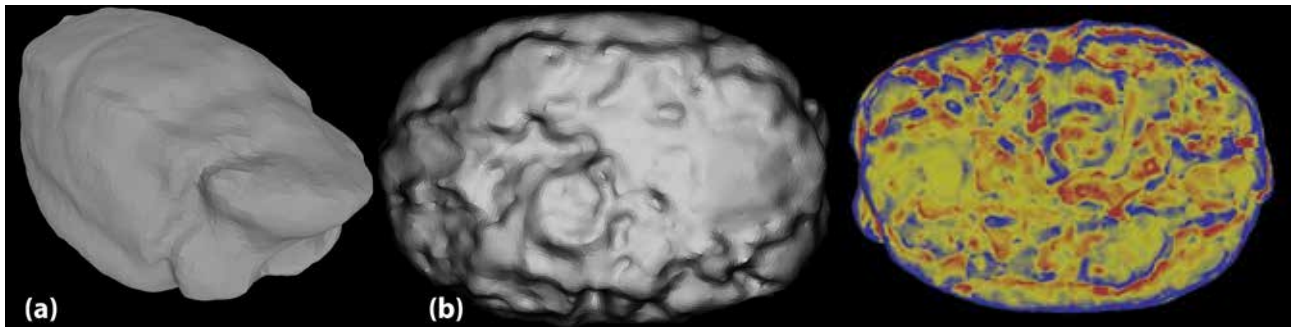


Fig. 49. a) 3D image of scarab N782 before the natural disintegration and 3D visualization of its base in MeshLab, by applying b) "Minnaert" and c) "Radiance scaling" shaders (copyrights: Valentina Vassallo and Rahaf Orabi).

no inscriptions or engraved shapes but the result of the material corrosion (Fig. 49c).

## SUMMARY AND CONCLUSIONS

The technical examination of three scarabs, N732, N782 and N794, enabled the acquisition of preliminary information on their materials and shape, as well as to docu-

ment their state of preservation. The results show that two white scarabs (N794 and N732) are made of a material comprised of low-Z elements based on the results of XRF analysis, which could be steatite (magnesium silicate) or ivory/bone. Scarab N782 is made of a green copper-containing material such as glass or faience. The white scarabs are decorated with carvings. The comparison of the results for these two scarabs suggests their common production,

Element	Line	keV	KRatio	Wt%	At%	At Prop	ChiSquared
O	KA1	0.523	0.8526	84.60	91.59	1851.2	184.43
Mg	KA1	1.254	0.0042	0.82	0.58	11.8	1.77
Al	KA1	1.487	0.0040	0.57	0.37	7.4	9.59
Si	KA1	1.740	0.0941	10.60	6.54	132.1	53.78
S	KA1	2.307	0.0007	0.07	0.04	0.7	4.71
K	KA1	3.313	0.0000	0.00	0.00	0.0	1.02
Ca	KA1	3.691	0.0015	0.11	0.05	1.0	0.88
Fe	KA1	6.403	0.0014	0.10	0.03	0.6	0.60
Cu	KA1	8.046	0.0388	2.89	0.79	15.9	1.88
Pb	LA1	10.550	0.0026	0.24	0.02	0.4	0.59
<b>Total</b>			<b>1.0000</b>	<b>100.00</b>	<b>100.00</b>	<b>2021.2</b>	<b>10.56</b>

Table 18. SEM-EDS elemental analysis of the green material of scarab N782.

Element	Line	keV	KRatio	Wt%	At%	At Prop	ChiSquared
C	KA1	0.277	0.7664	59.61	68.23	1182.3	89.86
O	KA1	0.523	0.1204	35.31	30.34	525.7	6.22
Al	KA1	1.487	0.0019	0.13	0.07	1.2	0.72
Si	KA1	1.740	0.0200	1.10	0.54	9.3	2.62
Cl	KA1	2.622	0.0006	0.03	0.01	0.2	0.93
Sb	LA1	3.604	0.0090	0.37	0.04	0.7	1.61
Ca	KA1	3.691	0.0042	0.17	0.06	1.0	1.36
V	KA1	4.951	0.0008	0.03	0.01	0.2	0.62
Tb	LA1	6.272	0.0008	0.04	0.00	0.1	0.78
Fe	KA1	6.403	0.0097	0.39	0.10	1.7	0.88
Cu	KA1	8.046	0.0659	2.82	0.61	10.6	1.84
<b>Total</b>			<b>1.0000</b>	<b>100.00</b>	<b>100.00</b>	<b>1732.9</b>	<b>1.72</b>

Table 19. SEM-EDS elemental analysis of the white material inside scarab N782.

indicating a standardization by the same hand or the same environment.

The poor state of preservation of the green scarab did not allow extraction of any information on its carved decoration. No deliberately applied painted decoration was detected on any of the scarabs. The presented data on micro-samples from the green scarab, as well as its 3D complete model before the degradation, could be used for future analysis of the scarab's production technique and comparison with similar scarabs reported in the literature.

## Bibliography

- Açkel, H., S. Ibiş & E. Şen Tunç 2018. 'Primary fused teeth and findings', *Permanent Dentition, Medical Principles and Practice* 27:2, 129–132.  
<https://doi.org/10.1159/000487322>
- AlQahtani, S.J. 2008. *Atlas of tooth development and eruption*, London.  
[www.atlas.dentistry.qmul.ac.uk](http://www.atlas.dentistry.qmul.ac.uk)
- Åström, P., ed. 1972. *The Swedish Cyprus Expedition* vol. IV:1C. *The Late Cypriote Bronze Age. Architecture and pottery*, Lund.
- Åström, P. 1983. 'Chamber tombs', in *Hala Sultan Tekke* vol. 8. *Excavations 1971–1979* (SIMA, 45:8), eds. P. Åström, E. Åström, A. Hatziantoniou, K. Niklasson & U. Öbrink, Gothenburg, 145–168.

- Bello, S. & P. Andrews 2006. 'The intrinsic pattern of preservation of human skeletons and its influence on the interpretation of funerary behaviours', in *Social archaeology of funerary remains*, eds. R.L. Gowland & C.J. Knüsel, Oxford, 1–13.
- Benson, J.L. 1972. *Bamboula at Kourion. The Necropolis and the finds*, Philadelphia.
- Bergoffen, C.J. 2005. *The Cypriot Bronze Age pottery from Sir Leonard Woolley's excavations at Alalakh (Tell Atchana)* (Contributions to the Chronology of the Eastern Mediterranean, 5), Vienna. <https://doi.org/10.1553/0x00071574>
- Brooks, S. & J.M. Suchey 1990. 'Skeletal age determination based on the os pubis. A comparison of the Acsádi-Nemeskéri and Suchey-Brooks methods', *Human Evolution* 5:3, 227–238. <https://doi.org/10.1007/BF02437238>
- Buikstra, J.E. & D.H. Ubelaker 1994. *Standards for data collection from human skeletal remains*, Fayetteville, Arkansas.
- Bürge, T. 2021. 'Mortuary landscapes revisited. Dynamics of insularity and connectivity in mortuary ritual, feasting, and commemoration in Late Bronze Age Cyprus', *Religions* 12:10, 877. <https://doi.org/10.3390/rel12100877>
- Cignoni, P., M. Callieri, M. Corsini, M. Dellepiane, F. Ganovelli & G. Ranzuglia 2008. 'MeshLab. An open-source mesh processing tool', in *Eurographics Italian Chapter Conference*, eds. V. Scarano, R.D. Chiara, U. Erra, Eindhoven, 129–136. <http://dx.doi.org/10.2312/LocalChapterEvents/ItalChap/ItalianChapConf2008/129-136>
- Edgar, H.J.H. 2017. *Dental morphology for anthropology. An illustrated manual*, New York.
- Eggler, J. & O. Keel 2006. *Corpus der Siegel-Amulette aus Jordanien. Vom Neolithikum bis zur Perserzeit* (Orbis Biblicus et Orientalis. Series Archaeologica, 25), Freiburg, Switzerland & Göttingen. <https://doi.org/10.5167/uzh-137127>
- Fischer, P.M. 1980. *Applications of technical devices in archaeology. The use of X-rays, microscope, electrical and electro-magnetic devices and subsurface interface radar* (SIMA, 63), Gothenburg.
- Fischer, P.M. 2003. 'The preliminary chronology of Tell el-ʿAjjul. Results of the renewed excavations in 1999 and 2000', in *The synchronisation of civilisations in the Eastern Mediterranean in the second millennium B.C. II. Proceedings of the SCIEEM 2000—Euro-Conference, Haindorf, 2nd of May–7th of May 2001* (Contributions to the Chronology of the Eastern Mediterranean, 4), ed. M. Bietak, Vienna, 263–294.
- Fischer, P.M. 2013. *Tell Abu al-Kharaz in the Jordan Valley* vol. 3. *The Iron Age* (Contributions to the Chronology of the Eastern Mediterranean, 34), Vienna.
- Fischer, P.M. & T. Bürge 2015. 'The New Swedish Cyprus Expedition 2014: Excavations at Hala Sultan Tekke. Preliminary Results', *OpAthRom* 8, 27–79. <https://doi.org/10.30549/opathrom-08-03>
- Fischer, P.M. & T. Bürge 2017. 'Tombs and offering pits at the Late Bronze Age metropolis of Hala Sultan Tekke, Cyprus', *BASOR* 377, 161–218. <https://doi.org/10.5615/bullamerschoorie.377.0161>
- Fischer, P.M. & T. Bürge 2018a. *Two Late Cypriot city quarters at Hala Sultan Tekke. The Söderberg Expedition 2010–2017* (SIMA, 147), Uppsala.
- Fischer, P.M. & T. Bürge 2018b. 'The New Swedish Cyprus Expedition 2017: Excavations at Hala Sultan Tekke (The Söderberg Expedition). Preliminary results', *OpAthRom* 11, 29–79. <https://doi.org/10.30549/opathrom-11-03>
- Fischer, P.M. & T. Bürge 2019. 'The New Swedish Cyprus Expedition 2018: Excavations at Hala Sultan Tekke (The Söderberg Expedition). Preliminary Results', *OpAthRom* 12, 287–326. <https://doi.org/10.30549/opathrom-12-10>
- Fischer, P.M. & T. Bürge 2020. 'The New Swedish Cyprus Expedition 2019: Excavations at Hala Sultan Tekke (The Söderberg Expedition). Preliminary results', *OpAthRom* 13, 73–111. <https://doi.org/10.30549/opathrom-13-03>
- Fischer, P.M. & T. Bürge 2021. 'The New Swedish Cyprus Expedition 2020 (The Söderberg Expedition): Excavations in the cemetery of Hala Sultan Tekke', *Ägypten und Levante* 31, 97–145. <https://doi.org/10.1553/AEundL31s97>
- Fischer, P.M. & T. Bürge 2022. 'The New Swedish Cyprus Expedition 2020 (The Söderberg Expedition): Excavations at Hala Sultan Tekke 2020 and 2021', *OpAthRom* 15, 7–76. <https://doi.org/10.30549/opathrom-15-02>
- Fletcher P.J., I. Freestone & R. Geschke 2008. 'Analysis and conservation of a weeping glass scarab', *British Museum Technical Research Bulletin* 2, 45–48.

- Georgopoulos, A., C. Ioannidis & A. Valanis 2010. 'Assessing the performance of a structured light scanner', in *International archives of photogrammetry, remote sensing and spatial information sciences* vol. 38:5, Newcastle upon Tyne, 250–255.
- Gjerstad, E. 1926. *Studies on Prehistoric Cyprus*, Uppsala.
- Gjerstad, E., J. Lindros, E. Sjöqvist & A. Westholm 1934. *The Swedish Cyprus Expedition. Finds and results of the Excavations in Cyprus 1927–1931* vol. 1, Stockholm.
- Graziadio, G. 2017. *The earliest production of Aegean-type pottery in Cyprus*, Pisa.
- Hall, H.R. 1913. *Catalogue of Egyptian scarabs, etc., in the British Museum* vol. 1. *Royal scarabs*, London.
- Hillson, S. 2005<sup>2</sup>. *Teeth*, Cambridge.  
<https://doi.org/10.1017/CBO9780511614477>
- Höflmayer, F. 2012. 'Ägyptische Imitationen zyprischer Base-Ring-Krüge im östlichen Mittelmeerraum. Ein Beispiel für Kulturkontakt im zweiten Jahrtausend v. Chr.', *Zeitschrift für Orient-Archäologie* 5, 210–231.
- Karageorghis, V. 1965. 'A Late Cypriote tomb at Tamassos', *RDAC* 1965, 11–29.
- Keel O. 1994. *Studien zu den Stempelsiegeln aus Palästina/Israel* vol. 4. *Mit Registern zu den Bänden I–IV* (Orbis Biblicus et Orientalis, 135), Freiburg, Switzerland & Göttingen.  
<https://doi.org/10.5167/uzh-141749>
- Keel, O. 1995. *Corpus der Stempelsiegel-Amulette aus Palästina/Israel. Von den Anfängen bis zur Perserzeit. Einleitung* (Orbis Biblicus et Orientalis. Series Archaeologica, 10), Freiburg, Switzerland & Göttingen.  
<https://doi.org/10.5167/uzh-142326>
- Keel, O. 1997. *Corpus der Stempelsiegel-Amulette aus Palästina/Israel. Von den Anfängen bis zur Perserzeit. Katalog* vol. 1. *Von Tell Abu Farağ bis Atlit* (Orbis Biblicus et Orientalis. Series Archaeologica, 13), Freiburg, Switzerland & Göttingen.  
<https://doi.org/10.5167/uzh-142340>
- Keel, O. 2010a. *Corpus der Stempelsiegel-Amulette aus Palästina/Israel. Von den Anfängen bis zur Perserzeit. Katalog* vol. 2. *Von Bahan bis Tel Eton* (Orbis Biblicus et Orientalis. Series Archaeologica, 29), Freiburg, Switzerland & Göttingen.  
<https://doi.org/10.5167/uzh-137116>
- Keel, O. 2010b. *Corpus der Stempelsiegel-Amulette aus Palästina/Israel. Von den Anfängen bis zur Perserzeit. Katalog* vol. 3. *Von Tell el-Farā-Nord bis Tell el-Fir* (Orbis Biblicus et Orientalis. Series Archaeologica, 31), Freiburg, Switzerland & Göttingen.  
<https://doi.org/10.5167/uzh-136930>
- Keel, O. 2013. *Corpus der Stempelsiegel-Amulette aus Palästina/Israel. Von den Anfängen bis zur Perserzeit. Katalog* vol. 4. *Von Tel Gamma bis Chirbet Husche* (Orbis Biblicus et Orientalis. Series Archaeologica, 33), Freiburg, Switzerland & Göttingen.  
<https://doi.org/10.5167/uzh-136778>
- Keel, O. 2017. *Corpus der Stempelsiegel-Amulette aus Palästina/Israel. Von den Anfängen bis zur Perserzeit. Katalog* vol. 5. *Von Tell el-Idham bis Tel Kitan* (Orbis Biblicus et Orientalis. Series Archaeologica, 35), Freiburg, Switzerland & Göttingen.  
<https://doi.org/10.5167/uzh-152239>
- Keswani, P. 2004. *Mortuary ritual and society in Bronze Age Cyprus* (Monographs in Mediterranean Archaeology, 9), London.
- Kozal, E. 2015. 'A discussion of the origin and the distribution patterns of Red Lustrous Wheel-made ware in Anatolia. Cultural connections across the Taurus and Amanus Mountains', in *La Cappadoce méridionale de la préhistoire à la période byzantine. 3èmes Rencontres d'Archéologie de l'IFÉA—Institut Français d'Études Anatoliennes Georges Dumézil, Istanbul 8–9 Novembre, 2012*, eds. D. Beyer, O. Henry & A. Tibet, Istanbul, 53–64.  
<https://doi.org/10.4000/books.ifeagd.3248>
- Kozal, E. 2023. 'Cypro-Anatolian connections en route to the downfall of the Late Bronze Age. An archaeological perspective from the 13th century BC', in *The decline of Bronze Age civilisations in the Mediterranean. Cyprus and beyond* (SIMA, 154), eds. T. Bürge & P.M. Fischer, Nicosia, 201–228.
- Lorentz, K.O. 2006. 'Human skeletal remains from the 1999 and 2000 seasons', in *Marki Alonia. An Early and Middle Bronze Age town in Cyprus. Excavations 1996–2000* (SIMA, 123:2), eds. D. Frankel & J. Webb, Jonsered, 293–297.
- Lorentz, K.O., S.A.M. Lemmers, C. Chrysostomou, W. Dirks, M.R. Zaruri, F. Foruzanfar & S.M.S. Sajjadi 2019. 'Use of dental microstructure to investigate the role of prenatal and early life physiological stress in age at death', *JAS* 104, 85–96.  
<https://doi.org/10.1016/j.jas.2019.01.007>

- Lorentz, K.O., N.M. Branca & S.A.M. Lemmers 2021a. 'Majewski/Microcephalic osteodysplastic primordial dwarfism type II (MOPDII) with generalised microdontia in the 4th millennium BCE Eastern Mediterranean', *International Journal of Paleopathology* 33, 158–169.  
<https://doi.org/10.1016/j.ijpp.2021.04.001>
- Lorentz, K.O., B. Casa & Y. Miyauchi 2021b. 'Disposed young. Nonadult element representation and bone positioning in complex mortuary programmes in Chalcolithic Cyprus', *International Journal of Osteoarchaeology* 31:5, 727.  
<https://doi.org/10.1002/oa.2985>
- Lorentz, K.O., S.A.M. Lemmers, C. Chrysostomou, W. Dirks, M.R. Zaruri, F. Foruzanfar & S.M.S. Sajjadi 2021c. 'First permanent molars with accentuated line patterns. Assessment of childhood health in an urban complex of the fifth millennium before the present', in *Archives of Oral Biology* 123, 104969.  
<https://doi.org/10.1016/j.archoralbio.2020.104969>
- Lovejoy, C.O. 1985. 'Dental wear in the Libben population. Its functional pattern and role in the determination of adult skeletal age at death', *American Journal of Physical Anthropology* 68:1, 47–56.  
<https://doi.org/10.1002/ajpa.1330680105>
- Lovejoy, C.O., R.S. Meindl, T.R. Pryzbeck & R.P. Mensforth 1985. 'Chronological metamorphosis of the auricular surface of the ilium. A new method for the determination of adult skeletal age at death', *American Journal of Physical Anthropology* 68:1, 15–28.  
<https://doi.org/10.1002/ajpa.1330680103>
- Meadows, L. & R.L. Jantz 1992. 'Estimation of stature from metacarpal lengths', *Journal of Forensic Sciences* 37:1, 147–154.
- Murray, A.S., A.H. Smith & H.B. Walters 1900. *Excavations in Cyprus*, London.
- Niklasson, K. 1983. 'Tomb 23. A shaft-grave of the Late Cypriote III period', in *Hala Sultan Tekke* vol. 8. *Excavations 1971–1979* (SIMA, 45:8), eds. P. Åström, E. Åström, A. Hatziantoniou, K. Niklasson & U. Öbrink, Gothenburg, 169–213.
- Petruso, K.M. 1984. 'Prolegomena to Late Cypriot weight metrology', *AJA* 88:3, 293–304.  
<https://doi.org/10.2307/504553>
- Pulak, C. 2000. 'The balance weights from the Late Bronze Age shipwreck at Uluburun', in *Metals make the world go round. The supply and circulation of metals in Bronze Age Europe. Proceedings of a conference held at the University of Birmingham in June 1997*, ed. C.F.E. Pare, Oxford, 247–266.
- Robb, J. 2016. 'What can we really say about skeletal part representation, MNI and funerary ritual? A simulation approach', *JAS Reports* 10, 684–692.  
<https://doi.org/10.1016/j.jasrep.2016.05.033>
- Rogers, N.L., L.E. Flournoy & W.F. McCormick 2000. 'The rhomboid fossa of the clavicle as a sex and age estimator', *Journal of Forensic Sciences* 45:1, 61–67.
- Schaefer, M., S. Black & L. Scheuer 2009. *Juvenile osteology. A laboratory and field manual*, Amsterdam.  
<https://doi.org/10.1016/B978-0-12-374635-1.X0001-X>
- Schirmer, W. 1998. 'Havara on Cyprus—a surficial calcareous deposit', *E&G Quaternary Science Journal* 48, 110–117.  
<https://doi.org/10.3285/eg.48.1.11>
- Schour, I. & M. Massler 1941. 'The development of the human dentition', *Journal of the American Dental Association* 28, 1153–1160.
- Sjøvold, T. 1990. 'Estimation of stature from long bones utilizing the line of organic correlation', *Human Evolution* 5:5, 431–447.  
<https://doi.org/10.1007/BF02435593>
- Soxman, J.A., P.B. Wunsch & C.M. Haberland 2019. *Anomalies of the developing dentition. A clinical guide to diagnosis and management*, Cham, 7–14.  
[https://doi.org/10.1007/978-3-030-03164-0\\_2](https://doi.org/10.1007/978-3-030-03164-0_2)
- Trotter, M. 1970. 'Estimation of stature from intact long limb bones', in *Personal identification in mass disasters*, ed. T.D. Stewart, Washington, 71–83.  
<https://doi.org/10.5479/sil.30678.39088001440254>
- Tufnell, O. 1953. *Lachish III (Tell ed-Duweir). The Iron Age*, 2 vols., London.
- Tufnell, O. 1958. *Lachish IV (Tell ed-Duweir). The Bronze Age*, 2 vols., London.
- Waldron, T. 2009. *Paleopathology*, Cambridge.
- Webb, J.M. 2018. 'Spatial and social discontinuities in burial practice and the privatisation of mortuary space in Bronze Age Cyprus', *JMA* 31:2, 203–228.  
<https://doi.org/10.1558/jma.38083>